Mir-214 and mir-148b targeting inhibits dissemination of melanoma and breast cancer

Inhibition of melanoma and breast cancer dissemination *in vivo* by targeting miR-214 and miR-148b

Francesca Orso[1,2,3*], Lorena Quirico[1,2*], Federico Virga[1,2], Elisa Penna[1,2], Daniela Dettori[1,2], Daniela Cimino[1,2,3], Roberto Coppo[1,2], Elena Grassi[1,2], Angela Rita Elia[1], Davide Brusa[4,5], Silvia Deaglio[4,5], Maria Felicia Brizzi[6], Michael B. Stadler[7], Paolo Provero[1,2], Michele Caselle[3,8] and Daniela Taverna[1,2,3]

[1]Molecular Biotechnology Center (MBC), [2]Dept. Molecular Biotechnology and Health Sciences, [3]Center for Complex Systems in Molecular Biology and Medicine, University of Torino, Torino, Italy; [4]Department of Medical Sciences, University of Torino, Torino, Italy; [5]Immunogenetics Unit, Human Genetics Foundation, Torino, Italy; [6]Department of Medical Sciences, University of Torino, Torino, Italy, [7]Friederich Miescher Institute and Swiss Institute of Bioinformatics, Basel, Switzerland; [8]Dept. of Physics University of Torino, Torino, Italy.

Running title: miR-214 and miR-148b targeting in tumor progression

Conflict of interest statement: the authors declare no competing financial interests

Character count: 5000??

*These authors contributed equally

Corresponding author:

Daniela Taverna
MBC and Dept. Molecular Biotechnology and Health Sciences,
University of Torino,
Via Nizza, 52,
10126 Torino, Italy
phone: +39 011 670 6497
fax: +39 011 670 6432
daniela.taverna@unito.it

ABSTRACT

MicroRNAs (miRNAs) are small non-coding RNAs that act as negative regulators of gene expression and play a central role in tumor progression. We previously unraveled the pro-metastatic function of miR-214 in melanoma and proved that miR-214-dependent tumor progression occurs by suppressing the anti-metastatic miR-148b. Here, we show that dissemination of melanoma and breast tumor cells in mice can be significantly impaired when cells are depleted of miR-214 or when miR-148b levels are increased. Relevantly, inhibition of metastasis formation is more evident when miR-214 and miR-148b are simultaneously altered in tumor cells. Furthermore, we prove that miR-214 depletion and miR-148b overexpression negatively control dissemination by suppressing the passage of malignant cells through the blood vessel endothelium due to ITGA5 and ALCAM expression reduction. In fact, transendothelial migration *in vitro* and extravasation *in vivo* are impaired following miR-214-negative and/or miR-148b-positive modulations, while transendothelial migration is re-established when ITGA5 or ALCAM are overexpressed in tumor cells. In line with these evidences, we found a positive correlation between miR-214 and ITGA5 or ALCAM in primary breast tumors and melanoma metastases while miR-214 and miR-148b anti-correlated in the same samples. In conclusion, we present evidences that miR-214 negative and miR-148b positive modulations inhibit tumor cell dissemination by blocking tumor-endothlelial cell interactions via ITGA5 and ALCAM, suggesting that these small RNAs can be considered valid targets for miRNA-based therapeutic interventions in tumor progression.

Words: 232 (max 250)

Key words: microRNA sponges / miR-214 / miR-148b / target genes / tumor progression

INTRODUCTION

Dissemination of primary tumor cells and the consequent formation of metastasis at distant organs are the main cause of cancer-related mortality. The currently available treatments for cancer (surgery, radio-, chemo- and targeted therapy) mainly control primary tumors, but they only exert a mild effect on metastases mostly because of resistance mechanisms activated by tumor cells. Therefore, it is crucial to identify key regulators of metastatic dissemination and to develop new targeted therapy approaches.

MicroRNAs (miRNAs) are small non-coding, single-stranded RNAs that act as negative regulators of gene expression. Increasing evidences show that deregulation of miRNAs is a crucial event in tumor progression. Several miRNAs, including miR-137, miR-221/222, miR-182, miR-34a and miR-214 have been found to be involved in melanoma malignancy by regulating key genes such as c-KIT, MITF, FOXO3, ITGB3, CCND1, p27Kip1, TFAP2 and ALCAM (1-3). Instead, let-7, miR-9, miR-10b, miR-21, miR-31, miR-146, miR-148b, miR-155, miR-200, miR-221/222 are main players in breast cancer dissemination (4-6). Therefore, it is essential to identify new miRNAs and understand how these small non-coding RNAs control the various steps of tumor malignancy and how they interact with one another to attempt miR-targeted therapies that can affect the molecular pathways involved in tumor progression. Several clinical trials based on the use of miRNA modulators in tumorigenesis have already been established (7).

We previously demonstrated that miR-214 promotes melanoma metastasis dissemination by increasing migration, invasion, extravasation and survival of melanoma cells via a novel pathway involving the metastasis suppressors, transcription modulators, TFAP2 (3). On the other hand, we found that miR-148b opposes breast cancer progression, acting directly on

the integrin signaling players ITGA5, ROCK1 and PIK3CA/p110α (6). More recently, we showed that miR-214 downregulates miR-148b in tumor cells via TFAP2C with the consequent upregulation of miR-148b direct targets (2). In order to explore the relevance of miR-214 and miR-148b for miR-based therapeutic interventions in melanoma and breast cancer, we analyzed the dissemination of miR-214-depleted and miR148b-overexpressing cells in mice, investigated how these small-RNAs influence cell metastatic traits and look for the main molecular players involved in this process. We demonstrated that single or combined modulations of miR-214 (inhibition) and miR148b (overexpression) significantly inhibit metastatization when tumor cells cross the vessel endothelium by decreasing the expression of ITGA5 and ALCAM, two adhesion molecules respectively involved in tumor-ExtraCellular Matrix (ECM) and cell-cell interactions.

MATERIALS AND METHODS

Cell culture

MA-2 and MC-1 cells were kindly provided by L. Xu and R.O. Hynes (8) and maintained as described in (2,3). Human HBL-100 were from American Type Culture Collection instead 4175-TGL and SK-MEL-28 were kindly provided respectively by J. Massagué (9) and L. Poliseno and maintained in standard conditions. Human umbilical vein endothelial cells (HUVECs) were kindly provided by L. Primo (with GFP) or generated by L. Brizzi and maintained as described in (2,3). All used cell lines were authenticated in the last 6 months by BMR Genomics (Padova, Italy), using the CELL ID System (Promega, Madison, WI).

Reagents and antibodies

miR precursors and inhibitors: Pre-miR™ miRNA Precursor Negative Control #1, Pre-miR™ miRNA Precursor Hsa-miR-214 (PM12124), Pre-miR™ miRNA Precursor hsa-miR-148b (PM10264), Anti-miR™ miRNA Inhibitor Negative Control #1, Anti-miR™ miRNA Inhibitor Hsa-miR-214 (AM12124), Anti-miR™ miRNA Inhibitor hsa-miR-148b (AM10264) (all from Applied Biosystems, Foster City, CA). TaqMan® MicroRNA assays for miRNA detection: Hsa-miR-214 ID 002306, Hsa-miR-148b ID 000471, U6 snRNA ID001973, U44 snRNA ID001904 (all from Applied Biosystems, Foster City, CA). Primary antibodies: anti-PIK3CA #4255 (Cell Signaling Technology, Danvers, MA), anti-GFP ab290 (Abcam, Cambridge, UK), anti-ITGA5 pAb RM10 kindly provided by G. Tarone, anti-CD166/ALCAM mAb MOG/07 (Novocastra Laboratories, Newcastle, UK), anti ROCK-1 pAb H-85, anti-hsp90 mAb F-8, anti-GAPDH pAb V-18, anti-ACTIN I-19 pAb (all from Santa Cruz Biotechnology, Santa Cruz, CA), anti-tubulin mAb B5-1-2 (Sigma, St Louis, MO), anti-CD31 pAb (Becton Dickinson, Pharmingen, NJ) . Secondary

antibodies: HRP-conjugated goat anti-mouse IgG, goat anti-rabbit IgG, donkey anti-goat IgG (all from Santa Cruz Biotechnology, Santa Cruz, CA), goat anti-rat IgG Alexa-Fluor-568 and goat anti-rat IgG Alexa-Fluor-488 (Molecular Probes, Invitrogen Life Technologies, Carlsbad CA). siRNAs: si ITGA5 (Hs_ITGA5_5 siRNA), si ALCAM (Hs_ALCAM_5 siRNA) and All Stars Negative Control siRNA were purchased from Qiagen (Stanford, CA, USA).

Sponge design and recombinant vector preparations

miR-214-sponges were described in (3). miR148b specific sponge sequences containing eight miRNA binding sites interrupted by 15-nts spacers were designed to be perfectly complementary to miR-148b seed region, with a bulge position 9-12 to prevent undesired cleavage of the sponge RNA. Sponges were synthesized by DNA 2.0 (Menlo Park, CA), cloned into pJ241 plasmids, excised using flanking HindIII sites, blunted and subcloned into blunted BamHI and SalI sites, downstream of EGFP into pLenti CMV-GFP-Puro (658-5) vector (Addgene), giving rise to pLenti148-spongeA/B. Nucleotides (in Table S1) were verified by sequencing. pLemiR-empty, pLemiR-214 and pLemiR-148b expression vectors were described in (3,6). The same miR-148b expression cassette was also subcloned in pLenti4/V5 expression vector (kindly provided by Mike di Persio).

Transient transfections, vectors and generation of stable cell lines

To obtain transient anti-miR or pre-miR or siRNA expression, cells were plated at 50% confluency and immediately transfected using HiPerFect Transfection Reagent (QIAGEN, Stanford, CA), with 100 nM anti-miR, 75 nM pre-miR or 100 nM siRNA. For transient cDNA overexpression, cells were plated at 90% confluency and transfected 24h later using Lipofectamine^{TM}2000 reagent (Invitrogen Life Technologies, Carlsbad, CA). For ITGA5 or

ALCAM overexepression pEGFP-N3-ITGA5 (6) or pLVX-ALCAM (2) expression vectors were used. All stable cell lines were generated via lentiviral infection. Sponge vectors were obtained as described above. pLKO.1-shALCAM lentiviral vector was from Open Biosystems (RHS3979). Lentiviruses were produced by calcium phosphate transfection of 20 μg vector plasmid together with 15 μg packaging (pCMVdR8.74) and 6 μg envelope (pMD2.G-VSVG) plasmids in 293T cells, according to Trono's lab protocol (http://tronolab.epfl.ch) and supernatants were harvested 48h post-transfection.

Protein or RNA isolation, Immunoblotting, qRT-PCRs for miRNA detection, Proliferation assays

Total protein or RNA extracts, immunoblotting, qRT-PCRs and proliferation assays were performed as described in (2,3).

Migration, invasion and transendothelial migration transwell assays

To measure migration and matrigel invasion $7.5x10^4$ MA-2 or MC-1, $3x10^4$ HBL-100, $5x10^4$ 4175-TGL or SK-MEL-28 were seeded in serum-free medium in the upper chambers of cell culture transwells with 8.0 μm pore size membrane (BD Biosciences, NJ), pre-coated or not with 4 μg/well growth factor reduced matrigel (BD Biosciences, NJ) or in BioCoat™ Matrigel Invasion Chambers (Becton Dickinson, NJ). The lower chambers were filled with complete growth medium. After 18h, the migrated cells on the lower side of the membrane were fixed in 2.5% glutaraldehyde, stained with 0.1% crystal violet and photographed using an Olympus IX70 microscope. For transendothelial migration assay 10^5 HUVECs were seeded in complete medium in the upper part of transwell inserts with 5.0 μm pore size membrane (Costar, Corning Incorporated, NY) coated by fibronectin at 5 $\mu g/cm^2$ or 0.1% gelatin, and grown till confluency. Then, $5x10^4$ cells labeled with

CellTracker™ Orange CMRA or Green CMFDA (Molecular Probes, Invitrogen Life Technologies, Carlsbad, CA), were seeded onto the HUVECs monolayer. 20h later HUVECs and non-transmigrated cells were removed and the red or green fluorescent cells that migrated on the lower side of the membrane were fixed in 4% paraformaldheyde and photographed using Zeiss Axiovert200M microscope. Migration, invasion and transendothelial migration were evaluated by measuring the area occupied by migrated cells using the ImageJ software (http://rsbweb.nih.gov/ij/).

ALCAM localization imaging

2 x 10^5 HUVECs-GFP were seeded on coverslips coated with fibronectin at 5 $\mu g/cm^2$, and grown till confluency. Then, 5x10^4 ALCAM-overexpressing MA-2 cells (stably transduced with pLVX-ALCAM expressing vector) were seeded on the HUVECs-GFP monolayer. 24h later the co-cultures were fixed in cold methanol and immunostained for ALCAM protein. Briefly, samples were blocked with 5% BSA, incubated with anti-CD166/ALCAM mAb MOG/07 (Novocastra Laboratories, 1:100 dilution) for 2h, then with anti-mouse IgG Alexa-Fluor-568 for 45 min and finally mounted on microscope slides for analyses and photos, performed with Confocal Leica SP5 microscope.

***In vivo* tumor growth and metastasis assays**

All experiments performed with live animals complied with ethical care. For tumor growth, 5×10^6 MC-1 cells (in PBS) were subcutaneously injected into the flanks of 8-12 weeks-old NOD/SCID/IL2R_null (NSG) immunocompromised mice, animals dissected 4 weeks later and proteins extracted from tumors. For experimental metastasis assays 5x10^5 MA-2 or MC-1 or SK-MEL-28 or 3x10^5 4175-TGL cells were injected into the tail vein of 8-12 weeks-old SCID or NOD/SCID/IL2R_null (NSG) immunocompromised mice and the

animals were dissected 7 or 4 weeks later respectively. Green or red fluorescent lung metastases were evaluated and photographed in fresh lungs *in toto* using a Leica MZ16F fluorescence stereomicroscope. The number of metastases was measured on photographs using the ImageJ software (http://rsbweb.nih.gov/ij/). Micrometastases were evaluated on paraffin-embedded and haematoxylin & eosin (H&E)-stained slides, scanned with Panoramic Desk (3DHistech, Euroclone).

***In vivo* extravasation assay**

A total of $1.5x10^6$ MC-1 or MA-2 or SK-MEL-28 cells, previously labeled with CellTracker™ Orange CMRA (Molecular Probes, Invitrogen Life Technologies), were injected into the tail vein of 4-6-weeks old female NSG mice (Charles River Laboratories). 2 or 48 hours later, mice were sacrificed and 4% paraformaldehyde was injected into the trachea. Lungs were dissected and photographed *in toto* using a Leica MZ16F fluorescence stereomicroscope and red fluorescence was quantified 48 hours following injections using the ImageJ software (http://rsbweb.nih.gov/ij/). Lungs were embedded in OCT (Killik, BioOptica, IT), frozen, cryostat-cut in 6-mm thick sections. Localization of tumor cells, inside/outside the vessels, was evaluated on sections at a Zeiss AxioObserver microscope with the ApoTome Module (3), following blood vessels staining with an anti-CD31 primary antibody in immunofluorescence.

Human tumor correlation analyses

Normalized expression values for mRNA and miRNA in breast cancer were downloaded from the European Genome-phenome Archive (EGAS00000000122: EGAD00010000434, EGAD00010000438 , Dvinge, et al., 2013, Curtis et al., 2012), and 1302 samples used. Instead, for melanomas, expression values were downloaded from The Cancer Genome

Atlas (TCGA, https://tcga-data.nci.nih.gov/tcga/) and 352 samples used. All analyses were performed with R using the packages stats (lm) and ggplot2 (REFs…? H. Wickham. ggplot2: Elegant Graphics for Data Analysis. Springer-Verlag New York, 2009. - R Core Team (2016). R: A language and environment for statistical computing. R Foundation for Statistical Computing, Vienna, Austria.URL https://www.R-project.org/).

Statistical analysis

The results are shown as mean ± Standard Deviation (SD) or as mean ± Standard Error of Mean (SEM), as indicated, and two-tailed Student's t test was used for comparison. *=P<0.05; ** = P<0.01; ***= P<0.001 were considered to be statistically significant. ns= indicates a non-statistically significant p-value.

RESULTS

miR-214 depletion and miR-148b overexpression inhibit melanoma and breast cancer metastasis formation in mice.

High levels of miR-214 are found in malignant melanomas and breast tumors and promote metastatization in mice by regulating a complex network of players, in a negative or positive manner, including the down-regulation of the anti-metastatic miR-148b. Here, we evaluated the potential therapeutic value of miR-214 depletion and miR-148b overexpression in tumor progression in mice.

Specific miR-214 or miR-148b sponges A or B were bio-informatically designed, cloned at the 3' end of a Green Fluorescent Protein (GFP) expression cassette in lentivirus vectors as in Table S1, Fig. S1A and (3) and tested in MC-1 or MA-2 melanoma cells. Specifically, cells were transfected with pLenti-214-spongeA/B or pLenti-148b-spongeA/B or pLenti-empty (control) vectors together with precursors for miR-214 or miR-148b or controls (pre-miR-214 or pre-miR-148b or pre-control) and GFP levels evaluated in cells at the microscope (S1B, C), by Western Blot-WB- (S1D, E) or FACS analysis (S1F, G). As shown, all sponges were able to inhibit GFP expression, suggesting miR-214 or miR-148b binding to their complementary sequences.

MC-1 or MA-2 melanoma or 4175-TGL breast cancer cells were then transduced with lentiviruses expressing miR-214-sponges (pLenti-214-spongeA/B) or miR-148b (pLenti/V5-148b, pLemiR-148b) or with empty-controls (pLenti-empty, pLenti4/V5-empty, pLemiR-empty). Alternatively, MA-2 or SK-MEL-28 melanoma or 4175-TGL breast cancer cells were transduced with lentiviruses expressing miR-148b-sponges (pLenti-148b-spongeA/B) or miR-214 (pLemiR-214) or with empty-controls (pLenti-

empty, pLemiR-empty) to verify the mechanism in the opposite directions. miR-214 and miR-148b levels were evaluated by qRT-PCR analyses as shown in Fig. S2-5. Cells with the expected miR-214 or miR-148b modulations were injected in the tail vein of immunocompromised mice and metastasis dissemination was evaluated 4 to 7 weeks later by measuring the number/area of lung metastasis in H&E-stained lung or liver sections or the fluorescent (green or red) tumor cells present in the whole organs (Fig. 1A-C, Fig. S6A-D, Fig. S7A-D). Single miR-214 downmodulation or miR-148b overexpression significantly blocked metastasis dissemination for MC-1 or MA-2 melanoma or 4175-TGL breast cancer cells compared to controls. Relevantly, simultaneous depletion of miR-214 and increased levels of miR-148b further blocked tumor spreading of melanoma and breast tumor cells compared to single modulations suggesting an additive action. In parallel, single miR-214 overexpression or miR-148b downmodulation, or simultaneous double targeting, favoured melanoma or breast cancer cell dissemination compared to controls.

In conclusion, we can consider miR-214 and miR-148b as promising targets for miRNA-based therapeutic interventions in tumor progression.

miR-214 inhibition and miR-148b overexpression control specific tumor cell metastatic traits.

To understand which metastatic traits of melanoma (MA-2, MC-1 and SK-MEL-28) and normal or tumor breast (HBL-100 and 4175-TGL) cells were affected by depletion of miR-214 and overexpression of miR-148b, we evaluated proliferation, migration, invasion through matrigel and transendothelial migration on a HUVECs monolayer *in vitro*, following miR-214 and miR-148b modulations. Cells were either transduced with lentiviruses for the depletion (pLenti-214-spongeB, pLenti-148b-spongeB) or

overexpression (pLemiR-214, pLenti4/V5-148b) of miR-214 or miR-148b or with empty controls (pLemiR-empty, pLenti-empty, pLenti4/V5-empty) or transiently transfected with miRNA precursors (pre-miR-214, anti-miR-148b, pre/anti-control). miR-214 and miR-148b modulations were evaluated by qRT-PCR assays as shown in Fig. S2-5. Single or double modulations of miR-214 and miR-148b did not significantly affect proliferation compared to controls in any tested cell line (Fig. 2 and S8). Instead, modulations of miR-214 or miR-148b significantly affected migration, cell movement across a HUVECs monolayer (transendothelial migration) and invasion in matrigel compared to controls (Fig. 3, Fig. S9). Precisely, in all assays, cell movement was impaired in miR-214-depleted and miR-148b-overexpressing cells. Opposite results were observed when miR-214 was highly expressed in cells while miR-148b expression was reduced. Relevantly, in transendothelial migration assays, but generally not in migration or invasion analyses, combined miR-214 inhibition and miR-148b overexpression almost always led to additive effects, like for *in vivo* metastasis (Fig. 1), suggesting a combinatorial, specific effect of miR-214 and miR-148b at the level of tumor-endothelial cell interactions.

miR-214 depletion and miR-148b overexpression impair tumor cell extravasation in mice.

The effect of single or combined sponge-induced miR-214 depletion and miR-148b overexpression was investigated on *in vivo* cell extravasation of tumor cells. CMRA-labeled MC-1 or SK-MEL-28 cells stably expressing miR-214-sponge (pLenti-214-spongeB) or miR-148b (pLenti4/V5-148b) or control vectors (pLenti-empty or pLenti4/V5-empty) were injected in the tail vein of immunocompromised mice (Fig. 4, S10, pictures and graphs). Lodging to the lung vasculature was evaluated 2 hours post-injection (Fig. 4a-d, Fig. S10a-b) and no difference was observed among modified cells. Instead, a strong

decrease in early (48 hours post-injection) lung colonization was observed following single or combined sponge-driven miR-214 downmodulation and miR-148b overexpression compared to controls in MC-1 (Fig. 4e-h) or SK-MEL-28 (Fig. S10c-d) cells. To note that cells were localized inside blood vessels or associated with them at 2 hours, as shown in Fig. S10e-f. Instead, cells were found in the lung parenchyma at 48 hours (Fig. 4i-l and Fig. S10g-h). As for metastasis dissemination (Fig. 1) and transendothelial migration (Fig. 3), combined miR-214 inhibition and miR-148b overexpression led to additive effects, suggesting, once more, a combinatorial, specific effect of miR-214 and miR-148b at the level of tumor-endothelial cell interactions.

Depletion of miR-214 and overexpression of miR-148b affect the adhesion molecules ITGA5 and ALCAM.

With the goal to identify the molecular players involved in reduced cancer dissemination/extravasation by miR-214 depletion and miR-148b overexpression in tumor cells, expression of ITGA5 and ALCAM, two validated miR-148b direct targets, known to be highly relevant for tumor cell dissemination, was analyzed in cell cultures or in mouse subcutaneous tumors. Single or combined miR-214 depletion and miR-148b overexpression in melanoma (MA-2, MC-1, SK-MEL-28) and tumor breast (4175-TGL) cells were obtained following stable transduction of lentivirus vectors for the expression of miR-214-sponges (pLenti-214-spongeB) or miR-148b (pLenti4/V5-148b) or empty controls (pLenti-empty, pLenti4/V5-empty). Alternatively, HBL100 cells were transiently transfected with anti-miR-214, pre-miR-148b or pre/anti-controls (Fig. S11E). miR-214 and miR-148b alterations were evaluated by qRT-PCR analyses as in Fig. S2-5. Important reduction of ITGA5 or ALCAM expression was observed for single or combined miR-modulations. Additive inhibitions of ITGA5 and ALCAM by dual miR-214/miR-148b

interventions were rarely observed compared to single interventions (Fig. 5 and S11E). Considering the relevance of ITGA5 and ALCAM expression impairment for the inhibition of transendothelial migration following combined miR-214/miR148b alterations, as presented below (see next paragraph), we can speculate that the effects of additive miR-214/miR-148b changes occur specifically when tumor cells get in contact with endothelial cells. Alternatively, supplementary alterations of gene expression could be involved in the passage of tumor cells through the blood vessels. Opposite stable or transient modulations were obtained in the same cells listed above and in HBL-100 normal breast cells to further evaluate this mechanism. Here, cells were transduced with pLenti-148b-spongeA/B or pLemiR-214 or the relative empty controls (pLenti-empty, pLemiR-empty) or transiently transfected with anti-miR-148b or pre-miR-214 or anti/pre-control and modulations evaluated by qRT-PCR assays as in Fig. S2-5. Here, increased levels of ITGA5 and ALCAM and their downstream players ROCK1 and PIK3CA were observed (Fig. S11), thus reinforcing the importance of this pathway in miR-214/miR-148b-driven tumor dissemination.

Impairment of tumor dissemination by miR-214 depletion and miR-148b overexpression depends on ITGA5 and ALCAM expression inhibition.

In order to understand if reduction of ITGA5 or ALCAM was essential for miR-214/miR-148b driven extravasation inhibition, we modulated ITGA5 or ALCAM levels in presence of miR-214 depletion and miR-148b overexpression.

First, ITGA5 or ALCAM expression was inhibited by RNA interference in a transient (si-ITGA5 or si-ALCAM) or stable (sh-ALCAM) manner in MA-2 melanoma or 4175-TGL breast cancer cells and transendothelial migration or extravasation evaluated by comparison

with empty (si-control, sh-control) cells. As shown in Fig. S12, reduced levels of ITGA5 or ALCAM significantly impaired transendothelial migration (Fig. S12A,B) or lung extravasation, 48 hours post-injection (tail vein) in immunocompromised mice (Fig. S12C,D) compared to controls. Modulations of ITGA5 or ALCAM were evaluated by Western Blot analysis (Fig. S12). Tumor-endothelial cell contacts are shown in a confocal microscope image (Fig. S12E) in which red (ALCAM staining) MA-2 tumor cells were in contact with green (GFP expression) HUVECs. All these results suggest the relevance of ITGA5 and ALCAM in the control of tumor cell transendothelial migration or extravasation during tumor progression. At this point, ITGA5 or ALCAM were overexpressed in MC-1 or 4175-TGL cells previously transduced with pLenti-214-spongeB or pLenti4/V5-148b or pLenti-empty/pLenti4/V5-empty lentivirus vectors, in single or dual combinations, and cells used to evaluate transendothelial migration. Modulations of ITGA5 or ALCAM were evaluated by Western Blot analysis (Fig. 6). In all conditions, we observed increased transendothelial migration, compared to controls when ITGA5 or ALCAM was overexpressed in cells. Thus suggesting that inhibition of transendothelial migration, driven by miR-214-depletion and miR-148b-overexpression, depends on the reduction of these adhesion molecules in tumor cells. In fact, transendothelial migration inhibition is rescued when ITGA5 or ALCAM levels are increased.

Taken together, our results prove that that the negative targeting of miR-214 and/or the positive modulation of miR-148b impairs dissemination by acting on ITGA5 or ALCAM, two main players for tumor cell extravasation.

miR-214 expression correlates with ITGA5 and ALCAM levels, while it anticorrelates with miR-148b, in melanoma metastases and in primary breast tumors.

Breast cancer (….REFs…, n=1302) and melanoma metastases (The Cancer Genome Atlas, TCGA, https://tcga-data.nci.nih.gov/tcga/, n=352) datasets were used to evaluate miR-214, miR-148b, ITGA5 and ALCAM expression and to look for possible correlations or anticorrelations with one another. Relevantly, we found that miR-214 and miR-148b anticorrelate in melanoma metastases (p=7.91e-05) and in primary breast tumors (p=5.43e-08), while miR-214 significantly correlates with ITGA5 and ALCAM in both datasets. *P values* were the following: for melanoma metastases: ITGA5 (p=3.09e-24), ALCAM (p=2.69e-09); for primary breast tumors: ITGA5 (p=1.68e-23), ALCAM (p=9.27e-07). These results are therefore in line with our above-presented investigations, thus strengthening the link between miR-214, miR-148b, ITGA5 and ALCAM and its relevance in human tumor progression.

DISCUSSION

We previously demonstrated the pro-metastatic role of miR-214 (3) and its link with the anti-metastatic miR-148b (2). Here, we show that single or combined miR-214 inhibition and miR-148b overexpression in tumor cells strongly modulate metastasis formation by acting mainly during the passage across the vessel endothelium (transendothelial migration/extravasation), a metastatic trait which involves two direct miR-148b targets, the adhesion receptors ITGA5 and ALCAM, in a cell-fibronectin and cell-cell dependent manner. Our data suggest that miR-214 and miR-148b are valuable targets for miR-based targeted therapy.

miR-214 is highly expressed in malignant cutaneous and ocular melanomas (3,10,11) as well as in breast, osteosarcoma, ovary, pancreas, prostate and gastric cancers (12-18). In line with these findings, upregulation of miR-214 in various tumor cells increases metastasis formation (2,3,19-21). On the other hand, miR-148b is poorly expressed in melanomas and in breast, oral, gastric, pancreatic and hepatocellular carcinomas (1,6,22-25) and its modulation in tumor cell lines reveals its anti-metastatic function (6,22,26,27). Here, by modulating miR-214 and miR-148b, respectively in a negative and positive manner, we show that miR-214 and miR-148b are part of a miR-ON-miR regulatory axis where miR-214 favours tumor dissemination following the downregulation of miR-148b and the consequent upregulation of miR-148b direct targets ITGA5 and ALCAM. Similarly, recent investigations underline the relevance of multiple miR connections (miR-ON-miR) or of miRs and transcription factors (TFs) reciprocal regulations (miR-ON-TF-ON-miR). Examples are Lin28-let-7-miR-181 in megakaryocyte differentiation (28), miR-181b-FOS-miR-21 in glioma progression (29), miR-103/107-miR-200 in epithelial-to-mesenchymal transition (EMT) (30), miR-199a/miR-214-let-7b-miR-34a-miR-762-miR-

1915 in breast cancer metastasis (31). All these evidences open up the possibility to target multiple players of the same pathway and give hope for combined therapeutic interventions. In line with this hypothesis, it has recently been shown that the simultaneous systemic delivery of two small non-coding RNAs acting as tumor suppressors, miR-34 and let-7, leads to reduced non-small lung cancer growth (32).

We propose that the presented miR-214-ON-miR-148b regulatory axis controls tumor dissemination acting, in particular, when tumor cells cross the blood vessels endothelium, via the modulation of ITGA5 and ALCAM (8,33-38). In fact, the silencing of ALCAM or ITGA5 inhibits transendothelial migration *in vitro* and extravasation *in vivo*. More relevantly, when miR-214 is depleted and/or miR-148b overexpressed, transendothelial migration suppression can be overcome by ITGA5 or ALCAM upregulation, thus suggesting that these two adhesion molecules are essential modulators of tumor-endothelial cell interactions. These results are in line with the fact that ALCAM is a cell-to-cell adhesion receptor known to play a major role in mediating the interactions between endothelial and tumor or immune cells during transendothelial migration (39-41). Moreover, ALCAM was found to be involved in cell movement (42) and in the conversion of the pro-metastatic pro-MMP-2 to its active form in malignancy (43). On the other hand, modulations of integrin expression were associated with various metastatic phenotypes (34,44-46). In particular, increased ITGA5 expression has been observed in metastatic melanoma cell lines compared with primary ones (47), and survivin-dependent ITGA5 upregulation was shown to enhance motility of melanoma cells (48). In MDAMB231 breast cancer cells, expression of ITGA5 promoted lung metastasis in both spontaneous and experimental lung metastasis models (34). In breast and ovarian cancer patients, ITGA5 expression was shown to be predictive of metastasis and poor prognosis (6,46,49). ITGA5

has also been linked to extravasation, in fact, it has been shown that Cav1–Rho-GTPase-dependent control of cell extravasation depends on ITGA5 expression levels and inhibition of this regulatory axis impairs extravasation and survival of metastatic cells (50). The fact that high levels of ITGA5 and ALCAM correlate with miR-214 and that miR-214 expression anticorrelates with miR-148b in human breast and melanoma, tumors or metastases, further strengthen the importance of these players and their direct functional connections in tumorigenesis.

With particular relevance for targeted therapy, the evidence that single or combined miR-214 downregulation and miR-148b upregulation in tumor cells inhibit metastasis formation in mice, gives hope for a miR-based therapy. Due to the relevance of ALCAM and ITGA5 in the pathway presented here, one could even speculate to target these two adhesion molecules with specific antibodies, in addition to miR-targeting, to further affect metastasis formation. Considering that the main issue of the miR-based targeted therapy is the *in vivo* delivery, it is essential to identify safe, selective and efficient compound systemic deliveries. For this purpose, we are currently developing new tools to administer miR-214 inhibitors and miR-148b precursors to animals and test their efficacy on metastasis formation.

In conclusion, our data demonstrate that the cascade of events including miR-214, miR-148b, ALCAM and ITGA5 is controlling melanoma and breast cancer progression and it can be exploited for combinatorial therapeutic interventions.

ACKNOWLEDGEMENTS

This work was supported by grants from Compagnia di San Paolo, Torino, 2008.1054 (DT), Progetto di ricerca di Ateneo 2102/SanPaolo Torino CASMATEN12 (MC), AIRC 2010, 2013 (IG2010-10104DT; IG2013-14201DT), Fondazione Cassa di Risparmio Torino CRT (2014.1085DT), and FIRB giovani 2008 (RBFR08F2FS-002 FO). EP was a FIRC fellow (2012–2014). PAOLO/MICHELE/ALTRI: volete aggiungere grants?

We are grateful to Lei Xu and Richard Hynes for the A375P cell line and its metastatic variants; Joan Massagué for the 4175-TGL cells; Laura Poliseno for the SK-MEL-28 cells; Luca Primo for the GFP-HUVECs; Mike Di Persio for the pLenti4/V5 expression vector; Jacek Krol for advices with the sponge constructs; Flavio Cristofani for his help with the immunocompromised mice and Marco Forni for pictures of histological sections.

REFERENCES (TO COMPLETE)

1. Mueller DW, Rehli M, Bosserhoff AK. miRNA expression profiling in melanocytes and melanoma cell lines reveals miRNAs associated with formation and progression of malignant melanoma. J Invest Dermatol 2009;129(7):1740-51.
2. Penna E, Orso F, Cimino D, Vercellino I, Grassi E, Quaglino E, et al. miR-214 coordinates melanoma progression by upregulating ALCAM through TFAP2 and miR-148b downmodulation. Cancer Res 2013;73(13):4098-111.
3. Penna E, Orso F, Cimino D, Tenaglia E, Lembo A, Quaglino E, et al. microRNA-214 contributes to melanoma tumour progression through suppression of TFAP2C. EMBO J 2011;30(10):1990-2007.
4. Shi M, Liu D, Duan H, Shen B, Guo N. Metastasis-related miRNAs, active players in breast cancer invasion, and metastasis. Cancer Metastasis Rev 2010;29(4):785-99.
5. Le Quesne J, Caldas C. Micro-RNAs and breast cancer. Mol Oncol 2010;4(3):230-41.
6. Cimino D, De Pitta C, Orso F, Zampini M, Casara S, Penna E, et al. miR148b is a major coordinator of breast cancer progression in a relapse-associated microRNA signature by targeting ITGA5, ROCK1, PIK3CA, NRAS, and CSF1. FASEB J 2013;27(3):1223-35.
7. Chen Y, Gao DY, Huang L. In vivo delivery of miRNAs for cancer therapy: challenges and strategies. Adv Drug Deliv Rev 2015;81:128-41.
8. Xu L, Shen SS, Hoshida Y, Subramanian A, Ross K, Brunet JP, et al. Gene expression changes in an animal melanoma model correlate with aggressiveness of human melanoma metastases. Mol Cancer Res 2008;6(5):760-9.
9. Minn AJ, Gupta GP, Siegel PM, Bos PD, Shu W, Giri DD, et al. Genes that mediate breast cancer metastasis to lung. Nature 2005;436(7050):518-24.
10. Segura MF, Belitskaya-Levy I, Rose AE, Zakrzewski J, Gaziel A, Hanniford D, et al. Melanoma MicroRNA signature predicts post-recurrence survival. Clin Cancer Res 2010;16(5):1577-86.
11. Worley LA, Long MD, Onken MD, Harbour JW. Micro-RNAs associated with metastasis in uveal melanoma identified by multiplexed microarray profiling. Melanoma Res 2008;18(3):184-90.
12. Volinia S, Calin GA, Liu CG, Ambs S, Cimmino A, Petrocca F, et al. A microRNA expression signature of human solid tumors defines cancer gene targets. Proc Natl Acad Sci U S A 2006;103(7):2257-61.
13. Blenkiron C, Goldstein LD, Thorne NP, Spiteri I, Chin SF, Dunning MJ, et al. MicroRNA expression profiling of human breast cancer identifies new markers of tumor subtype. Genome Biol 2007;8(10):R214.
14. Sempere LF, Christensen M, Silahtaroglu A, Bak M, Heath CV, Schwartz G, et al. Altered MicroRNA expression confined to specific epithelial cell subpopulations in breast cancer. Cancer Res 2007;67(24):11612-20.
15. Ueda T, Volinia S, Okumura H, Shimizu M, Taccioli C, Rossi S, et al. Relation between microRNA expression and progression and prognosis of gastric cancer: a microRNA expression analysis. Lancet Oncol 2010;11(2):136-46.

16. Yang H, Kong W, He L, Zhao JJ, O'Donnell JD, Wang J, et al. MicroRNA expression profiling in human ovarian cancer: miR-214 induces cell survival and cisplatin resistance by targeting PTEN. Cancer Res 2008;68(2):425-33.
17. Wang Z, Cai H, Lin L, Tang M, Cai H. Upregulated expression of microRNA-214 is linked to tumor progression and adverse prognosis in pediatric osteosarcoma. Pediatr Blood Cancer 2014;61(2):206-10.
18. Wang M, Zhao C, Shi H, Zhang B, Zhang L, Zhang X, et al. Deregulated microRNAs in gastric cancer tissue-derived mesenchymal stem cells: novel biomarkers and a mechanism for gastric cancer. Br J Cancer 2014;110(5):1199-210.
19. Yang TS, Yang XH, Wang XD, Wang YL, Zhou B, Song ZS. MiR-214 regulate gastric cancer cell proliferation, migration and invasion by targeting PTEN. Cancer Cell Int 2013;13(1):68.
20. Xu Z, Wang T. miR-214 promotes the proliferation and invasion of osteosarcoma cells through direct suppression of LZTS1. Biochem Biophys Res Commun 2014;449(2):190-5.
21. Deng M, Ye Q, Qin Z, Zheng Y, He W, Tang H, et al. miR-214 promotes tumorigenesis by targeting lactotransferrin in nasopharyngeal carcinoma. Tumour Biol 2013;34(3):1793-800.
22. Song YX, Yue ZY, Wang ZN, Xu YY, Luo Y, Xu HM, et al. MicroRNA-148b is frequently down-regulated in gastric cancer and acts as a tumor suppressor by inhibiting cell proliferation. Mol Cancer 2011;10:1.
23. Yu ZW, Zhong LP, Ji T, Zhang P, Chen WT, Zhang CP. MicroRNAs contribute to the chemoresistance of cisplatin in tongue squamous cell carcinoma lines. Oral Oncol 2010;46(4):317-22.
24. Bloomston M, Frankel WL, Petrocca F, Volinia S, Alder H, Hagan JP, et al. MicroRNA expression patterns to differentiate pancreatic adenocarcinoma from normal pancreas and chronic pancreatitis. JAMA 2007;297(17):1901-8.
25. Zhang Z, Zheng W, Hai J. MicroRNA-148b expression is decreased in hepatocellular carcinoma and associated with prognosis. Med Oncol 2014;31(6):984.
26. Zhao G, Zhang JG, Liu Y, Qin Q, Wang B, Tian K, et al. miR-148b functions as a tumor suppressor in pancreatic cancer by targeting AMPKalpha1. Mol Cancer Ther 2013;12(1):83-93.
27. Liu GL, Liu X, Lv XB, Wang XP, Fang XS, Sang Y. miR-148b functions as a tumor suppressor in non-small cell lung cancer by targeting carcinoembryonic antigen (CEA). Int J Clin Exp Med 2014;7(8):1990-9.
28. Li X, Zhang J, Gao L, McClellan S, Finan MA, Butler TW, et al. MiR-181 mediates cell differentiation by interrupting the Lin28 and let-7 feedback circuit. Cell Death Differ 2012;19(3):378-86.
29. Tao T, Wang Y, Luo H, Yao L, Wang L, Wang J, et al. Involvement of FOS-mediated miR-181b/miR-21 signalling in the progression of malignant gliomas. Eur J Cancer 2013;49(14):3055-63.
30. Martello G, Rosato A, Ferrari F, Manfrin A, Cordenonsi M, Dupont S, et al. A MicroRNA targeting dicer for metastasis control. Cell 2010;141(7):1195-207.
31. Cuiffo BG, Campagne A, Bell GW, Lembo A, Orso F, Lien EC, et al. MSC-regulated microRNAs converge on the transcription factor FOXP2 and promote breast cancer metastasis. Cell Stem Cell 2014;15(6):762-74.
32. Kasinski AL, Kelnar K, Stahlhut C, Orellana E, Zhao J, Shimer E, et al. A combinatorial microRNA therapeutics approach to suppressing non-small cell lung cancer. Oncogene 2014.

33. van Kempen LC, van den Oord JJ, van Muijen GN, Weidle UH, Bloemers HP, Swart GW. Activated leukocyte cell adhesion molecule/CD166, a marker of tumor progression in primary malignant melanoma of the skin. Am J Pathol 2000;156(3):769-74.
34. Valastyan S, Benaich N, Chang A, Reinhardt F, Weinberg RA. Concomitant suppression of three target genes can explain the impact of a microRNA on metastasis. Genes Dev 2009;23(22):2592-7.
35. Liu S, Goldstein RH, Scepansky EM, Rosenblatt M. Inhibition of rho-associated kinase signaling prevents breast cancer metastasis to human bone. Cancer Res 2009;69(22):8742-51.
36. Lane J, Martin TA, Watkins G, Mansel RE, Jiang WG. The expression and prognostic value of ROCK I and ROCK II and their role in human breast cancer. Int J Oncol 2008;33(3):585-93.
37. Zheng B, Liang L, Wang C, Huang S, Cao X, Zha R, et al. MicroRNA-148a suppresses tumor cell invasion and metastasis by downregulating ROCK1 in gastric cancer. Clin Cancer Res 2011;17(24):7574-83.
38. Renner O, Blanco-Aparicio C, Grassow M, Canamero M, Leal JF, Carnero A. Activation of phosphatidylinositol 3-kinase by membrane localization of p110alpha predisposes mammary glands to neoplastic transformation. Cancer Res 2008;68(23):9643-53.
39. Swart GW, Lunter PC, Kilsdonk JW, Kempen LC. Activated leukocyte cell adhesion molecule (ALCAM/CD166): signaling at the divide of melanoma cell clustering and cell migration? Cancer Metastasis Rev 2005;24(2):223-36.
40. Weidle UH, Eggle D, Klostermann S, Swart GW. ALCAM/CD166: cancer-related issues. Cancer Genomics Proteomics 2010;7(5):231-43.
41. Masedunskas A, King JA, Tan F, Cochran R, Stevens T, Sviridov D, et al. Activated leukocyte cell adhesion molecule is a component of the endothelial junction involved in transendothelial monocyte migration. FEBS Lett 2006;580(11):2637-45.
42. van Kilsdonk JW, Wilting RH, Bergers M, van Muijen GN, Schalkwijk J, van Kempen LC, et al. Attenuation of melanoma invasion by a secreted variant of activated leukocyte cell adhesion molecule. Cancer Res 2008;68(10):3671-9.
43. Lunter PC, van Kilsdonk JW, van Beek H, Cornelissen IM, Bergers M, Willems PH, et al. Activated leukocyte cell adhesion molecule (ALCAM/CD166/MEMD), a novel actor in invasive growth, controls matrix metalloproteinase activity. Cancer Res 2005;65(19):8801-8.
44. Kuphal S, Bauer R, Bosserhoff AK. Integrin signaling in malignant melanoma. Cancer Metastasis Rev 2005;24(2):195-222.
45. Mierke CT, Frey B, Fellner M, Herrmann M, Fabry B. Integrin alpha5beta1 facilitates cancer cell invasion through enhanced contractile forces. J Cell Sci 2011;124(Pt 3):369-83.
46. Sawada K, Mitra AK, Radjabi AR, Bhaskar V, Kistner EO, Tretiakova M, et al. Loss of E-cadherin promotes ovarian cancer metastasis via alpha 5-integrin, which is a therapeutic target. Cancer Res 2008;68(7):2329-39.
47. McKenzie JA, Liu T, Goodson AG, Grossman D. Survivin enhances motility of melanoma cells by supporting Akt activation and {alpha}5 integrin upregulation. Cancer Res 2010;70(20):7927-37.
48. McKenzie JA, Liu T, Jung JY, Jones BB, Ekiz HA, Welm AL, et al. Survivin promotion of melanoma metastasis requires upregulation of alpha5 integrin. Carcinogenesis 2013;34(9):2137-44.

49. Mitra AK, Sawada K, Tiwari P, Mui K, Gwin K, Lengyel E. Ligand-independent activation of c-Met by fibronectin and alpha(5)beta(1)-integrin regulates ovarian cancer invasion and metastasis. Oncogene 2011;30(13):1566-76.
50. Arpaia E, Blaser H, Quintela-Fandino M, Duncan G, Leong HS, Ablack A, et al. The interaction between caveolin-1 and Rho-GTPases promotes metastasis by controlling the expression of alpha5-integrin and the activation of Src, Ras and Erk. Oncogene 2012;31(7):884-96.

FIGURE LEGENDS

Figure 1 - miR-214 depletion and miR-148b overexpression inhibit metastasis formation in mice.

Lung or liver colony formation in immunodeficient mice, 7 (A) or 4 (B, C) weeks after tail vein injection of MC-1 (A) or 4175-TGL (B, C) cells. Cells were transduced with controls (pLenti-empty, pLenti4/V5-empty) or miR-214-sponge (pLenti-214-spongeB) or miR-148b-overexpressing (pLenti4/V5-148b) vectors, single or in combination, as indicated in the panels. Representative pictures of H&E stained sections (A, B, a-d, bar=500 μm; C, a-d, bar=100 μm) are shown. Graphs (bottom of each figure) represent quantitated results as mean±SEM H&E stained colonies number (A) or as percentage of metastatic/total areas (B) in lungs or as mean metastases/field in liver, referring to the indicated number of mice (n). 2 independent experiments were performed and representative results are shown. SEM= Standard Error of Mean; H&E=Haematoxylin and Eosin.

Figure 2 - miR-214 depletion and miR-148b overexpression do not affect proliferation.

(A-C) Proliferation of MC-1 (A) or 4175-TGL (B) cells stably transduced with control (pLenti-empty, pLenti4/V5-empty) or miR-214-sponge (pLenti-214-spongeB) or miR-148b-overexpressing (pLenti4/V5-148b) vectors, single or in combination, as indicated in the graphs. Results are indicated as mean±SD of the proliferation ratio versus plated cells, measured by optical density at 0-72h. At least 2 independent experiments (with triplicates) were performed and representative results are shown. SD=Standard Deviation.

Figure 3 - miR-214 depletion and miR-148b overexpression inhibit transendothelial migration.

Transwell migration assays were used to evaluate migration (through a porous membrane) or transendothelial migration (through a HUVECs monolayer on top of a porous membrane) for MC-1 (A, B) or 4175-TGL (C, D) or SK-MEL-28 (E, F) cells stably transduced with control (pLenti-empty, pLenti4/V5-empty) or miR-214-sponge (pLenti-214-spongeB) or miR-148b-overexpressing (pLenti4/V5-148b) vectors, single or in combination, as indicated in the panels. For migration, results are indicated as ratio of mean±SEM of the area covered by migrated versus plated tumor cells, for transendothelial migration, results are shown as mean±SEM of the area covered by migrated cells. At least 2 independent experiments (with triplicates) were performed and representative results are shown. SEM= Standard Error of Mean.

Figure 4 - miR-214 depletion and miR-148b overexpression inhibit extravasation in mice.

In vivo extravasation 2h (a-d) or 48h (e-h) following tail vein injections in immunodeficient mice of CMRA-labeled MC-1 cells transduced with control (pLenti-empty, pLenti4/V5-empty) or miR-214-sponge (pLenti-214-spongeB) or miR-148b-overexpressing (pLenti4/V5-148b) vectors, single or in combination, as indicated in the panels. Representative pictures of whole red fluorescent lungs at 2h or 48h post-injection (a-h) and representative fields of murine lung sections, 48h post-injection (i-l), stained for CD31 (green) and counterstained with DAPI (blue) are shown; bar=800 μm. Results are indicated in the graphs (bottom) as mean±SEM of the number of extravasated cells at 48h for n=4 mice per group. White arrows indicate extravasated cells. 2 independent experiments were performed and representative results are shown. SEM= Standard Error of Mean.

Figure 5 - miR-214 depletion and miR-148b overexpression affect ITGA5 and ALCAM expression.

(A-D) Western blot analysis of ITGA5 or ALCAM protein expression levels in MC-1 (A), MC-1-SQ (B), 4175-TGL (C), SK-MEL-28 (D), transiently transfected with precursors for miR-148b (pre-miR-148b) or inhibitors for miR-214 (anti-miR-214) or negative controls (pre-control or anti-control) single or in combination or stably transduced with controls (pLenti-empty, pLenti4/V5-empty) or miR-214-sponge (pLenti-214-spongeB) or miR-148b-overexpressing (pLenti4/V5-148b) vectors, single or in combination, as indicated. Protein modulations were calculated relative to empty controls, normalized on loading controls (GAPDH or Actin or hsp90 or Tubulin) and expressed as percentages (%). 3 independent experiments were performed and representative ones are shown. SQ=subcutaneous tumors.

Figure 6 –Transendothelial migration depends on ITGA5 and ALCAM expression in miR-214-depleted and/or miR-148b-overexpressing tumor cells.

Transendothelial migration was evaluated in MC-1 or 4175-TGL cells stably transduced with miR-214-sponge (pLenti-214-spongeB) or miR-148b-overexpressing (pLenti4/V5-148b) vectors, single or in combination, and in addition, transiently transfected with recombinant vectors for the overexpression of ITGA5 or ALCAM or empty controls, as indicated in the panels (A-F). ITGA5 and ALCAM levels were evaluated by Western Blot analysis, 24h or 48h following transfections. Protein modulations were calculated relative to negative controls, normalized on loading controls (GAPDH or Actin) and expressed as percentages (%). Transmigration results are indicated as mean±SEM of the area covered by migrated cells. At least 2 independent experiments (with triplicates) were performed and representative results are shown. SEM= Standard Error of Mean.

Figure 7– miR-214 anti-correlates with miR-148b, while it correlates with miR-148b targets ITGA5 and ALCAM, in melanoma metastases or human primary breast tumors.

The indicated datasets were used to evaluate miR-214, miR-148b, ITGA5 and ALCAM expression in melanoma metastases (A) and in primary breast tumors (B). Statistically significant negative or positive correlations are shown for miR-214 and miR-148b (anticorrelations) and for miR-214 and ITGA5 or ALCAM (correlations). Correlations of normalized expression are represented with a dot-plot superimposing the regression line. The shaded area represents the 0.95 standard error confidence interval of the model predictions. Statistically significant R2 and P values and number of samples (n) are indicated.

SUPPLEMENTARY TABLES AND FIGURE LEGENDS

Table S1 – miR-214 and miR-148b sponge sequences

Figure S1 – Analysis of miR-214 and miR-148b sponge efficacy.

(A) Schematic representation of sponge constructs containing specific sites for miR-214 and miR-148b. (B, C) GFP expression in the indicated melanoma cell lines 48h after transfection of miR-214 (pLenti-214-spongeA/B) or miR-148b (pLenti-148b-spongeA/B) sponges alone or in combination with miR-214 (pre-miR-214) or miR-148b (pre-miR-148b) precursors or negative controls (pre-control). Cells were photographed using a Zeiss Axiovert200M microscope (B, a-i, C, a-i; bar=2 mm;). (D, E) Western Blot analysis of GFP protein expression levels in the indicated melanoma cells transfected as in (B, C). Protein modulations were calculated relative to controls, normalized on loading controls (hsp90) and expressed as percentages (%). (F, G) FACS analyses for GFP levels in the indicated melanoma cells transfected as in (B, C). At least 2 independent experiments were performed and representative results are shown.

Figure S2- miR-214 expression modulations in melanoma cells.

(A-E) miR-214 expression levels were tested by qRT-PCR analyses for the indicated melanoma cell lines stably transduced with control (pLenti-empty, pLenti4/V5-empty) or miR-214 sponges (pLenti-214-spongeA/B) or with miR-148b (pLenti4/V5-148b) overexpression vectors, alone or in combination. (F-J) Alternatively, cells were transiently transfected with miR-148b (anti-miR-148b) or miR-214 (anti-miR-214) inhibitors; miR-214 or miR-148b precursors (pre-miR-214 or pre-miR-148b) or negative controls (anti- or pre-control) alone or in combination, as indicated in the graphs. Results are shown as fold changes (mean±SD of triplicates) relative to controls, normalized on U6 or U44 small nucleolar RNA level.

Figure S3 - miR-214 expression modulations in normal or tumor breast cells.

(A-E) miR-214 expression levels were tested by qRT-PCR analyses for the indicated normal or tumor breast cell lines stably transduced with control (pLenti-empty, pLenti4/V5-empty or pLemiR-empty) or miR-214 (pLenti-214-spongeB) or miR-148b (pLenti-148b-spongeB) sponges or with miR-148b (pLenti4/V5-148b) or miR-214 (pLemiR-214) overexpression vectors alone or in combination. (F-I) Alternatively, cells were transiently transfected with miR-148b (anti-miR-148b) inhibitors or miR-214 precursors (pre-miR-214) or negative controls (anti- or pre-control), alone or in combination as indicated in the graphs. Results are shown as fold changes (mean±SD of triplicates) relative to controls, normalized on U6 or U44 small nucleolar RNA level.

Figure S4 - miR-148b expression modulations in melanoma cells.

(A-G) miR-148b expression levels were tested by qRT-PCR analyses for the indicated cell lines stably transduced with control (pLenti-empty, pLenti4/V5-empty or pLemiR-empty) or miR-214 (pLenti-214-spongeB) or miR-148b (pLenti-148b-spongeB) sponges or with miR-148b (pLemiR-148b or pLenti4/V5-148b) overexpression vectors alone or in combination. (H-M) Alternatively cells were transiently transfected with miR-148b (anti-miR-148b) or miR-214 (anti-miR-214) inhibitors; miR-214 or miR-148b precursors (pre-miR-214 or pre-miR-148b) or negative controls (anti- or pre-control) alone or in combination, as indicated in the graphs. Results are shown as fold changes (mean±SD of triplicates) relative to controls, normalized on U6 or U44 small nucleolar RNA level.

Figure S5 - miR-148b expression modulations in normal or tumor breast cells.

(A-D, I) miR-148b expression levels were tested by qRT-PCR analyses for the indicated cell lines stably transduced with control (pLenti-empty, pLenti4/V5-empty or pLemiR-empty) or miR-214 (pLenti-214-spongeB) or miR-148b (pLenti-148b-spongeA/B) sponges or with miR-148b

(pLenti4/V5-148b) or miR-214 (pLemiR-214) overexpression vectors alone or in combination. (E-H) Alternatively, cells were transiently transfected with miR-148b (anti-miR-148b) inhibitors or miR-214 precursors (pre-miR-214) or negative controls (anti- or pre-control) alone or in combination, as indicated in the graphs. Results are shown as fold changes (mean±SD of triplicates) relative to controls, normalized on U6 or U44 small nucleolar RNA level.

Figure S6 - miR-214 and miR-148b coordinate lung metastasis formation in an opposite manner.

Lung colony formation in immunodeficient mice, 7 (A) or 4 (B-D) weeks after tail vein injection of MC-1 (A), MA-2 (B, C), or 4175-TGL (D) cells. Cells were transduced as indicated in the panels: controls (pLenti-empty or pLemiR-empty) or miR-214-sponge (pLenti-214-spongeA/B) or miR-148b-sponge (pLenti-148b-spongeA/B) or miR-148b-overexpressing (pLemiR-148b) or miR-214-overexpressing (pLemiR-214) vectors, expressing GFP or tRFP. Representative pictures of green or red fluorescent whole lungs (A and C, a-c; B and D, a-b; bar=800 μm) or H&E stained sections (A and C, d-f; B and D, c-d, bar=200 μm) are shown. Graphs (bottom of each figure) represent quantitated results as mean±SEM of the number of fluorescent colonies in lungs, referring to the indicated number of mice (n). 2 independent experiments were performed and representative results are shown. SEM= Standard Error of Mean; H&E=Haematoxylin and Eosin.

Figure S7 - miR-148b reduces liver and lung metastasis formation.

Liver (A, B) and lung (C, D) colony formation in immunodeficient mice, 4 (A, B, D) or 7 (C) weeks after tail vein injection of MA-2 or SK-MEL-28 or 4175-TGL cells transduced with the following overexpressing vectors: control (pLenti-empty and/or pLemiR-empty) or miR-148b sponges (pLenti-148b-spongeA/B) or miR-148b (pLemiR-148b) or miR-214 (pLemiR-214), including GFP or tRFP expression or not, single or in combination. Representative pictures of fluorescent whole livers (A, a-b; B, a-c, bar=800 μm) or of H&E-stained lung sections are shown

(C, D a-b, bar=40 μm and 500 μm, respectively). Graphs (bottom of each figure) present quantitated results as mean±SEM of the number of fluorescent colonies in livers (A, B) or of the number of H&E colonies (C) or of the percentage of metastatic/total area in lungs (D) referring to the number of mice (n) indicated. 2 independent experiments were performed and representative results are shown. SEM= Standard Error of Mean.

Figure S8 - miR-214 and miR-148b do not significantly affect proliferation.

Proliferation of HBL-100 cells transiently transfected with miR-214 precursors (pre-miR-214) or miR-148b (anti-miR-148b) inhibitors or negative controls (pre- or anti-control) in single or in combination as indicated in the graphs. Results are indicated as mean±SD of the proliferation ratio versus plated cells, measured by optical density at 0-72h. At least 2 independent experiments (with triplicates) were performed and representative results are shown. SD=Standard Deviation.

Figure S9 - miR-214 and miR-148b affect migration and invasion ability.

Transwell migration (A-C) or invasion on matrigel (D-F) assays for HBL-100 (A), 4175-TGL (B), SK-MEL-28 (C, D), MC-1 (E) or MA-2 (F) cells transiently transfected with miR-214 precursors (pre-miR-214) or miR-148b inhibitors (anti-miR-148b) or negative controls (pre-control or anti-control), alone or in combination, or stably transduced with controls (pLenti-empty and/or pLenti4/V5-empty) or miR-214 (pLenti-214-spongeB) or miR-148b (pLenti-148b-spongeB) sponges or miR-148b-overexpressing (pLenti4/V5-148b) vectors, single or in combination, as indicated in the panels. Results are indicated as ratio mean±SEM of the area covered by migrated versus plated cells. At least 2 independent experiments (with triplicates) were performed and representative results are shown. SEM= Standard Error of Mean.

Figure S10 - miR-214 inhibition and miR-148b overexpression impair melanoma cell extravasation.

In vivo extravasation 2h (a, b) or 48h (c, d) following tail vein injections in immunosuppressed mice of CMRA-labeled SK-MEL-28 cells transduced with a combination of control (pLenti-empty, pLenti4/V5-empty) or miR-214-sponge (pLenti-214-spongeB) and miR-148b-overexpressing (pLenti4/V5-148b) vectors as indicated in the panels. Representative pictures of whole red fluorescent lungs are shown (a-d); bar=800 μm. Representative fields of murine lung sections 2h (e, f) or 48h (g, h) post-injections, stained for CD31 (red) and counterstained with DAPI (blue). Arrows indicate metastatic cells. Results are indicated in the graph (bottom) as mean±SEM of the fluorescence intensity at 48h for n=4 mice per group. 2 independent experiments were performed and representative results are shown. SEM= Standard Error of Mean.

Figure S11 - miR-148b target genes analysis.

(A-E) Western blot analysis of ALCAM, ITGA5, ROCK1 and PIK3CA protein expression levels in MA-2 or 4175-TGL or HBL-100 cells transiently transfected with miR-214 (pre-miR-214) or miR-148b (pre-miR-148b) precursors or miR-148b inhibitors (anti-miR-148b) or negative controls (anti- or pre-control), alone or in combination, or stably transduced with control (pLemiR-empty and/or pLenti-empty) or miR-214-overexpressing (pLemiR-214) or miR-148b-sponges (pLenti-148b-spongeA/B) vectors as indicated. Protein modulations were calculated relative to controls, normalized on loading controls (GAPDH or Actin or hsp90 or Tubulin) and expressed as percentages (%). 3 independent experiments were performed and representative ones are shown.

Figure S12 –ITGA5 and ALCAM control transendothelial migration *in vitro* and extravasation in mice.

(A-B) Transendothelial migration was evaluated in MA-2 (A) or 4175-TGL (B) cells transiently transfected with si-ITGA5 or si-ALCAM or control siRNAs (si-control) or transduced for sh-ALCAM or sh-control, as indicated in the panels (A, B). ITGA5 and ALCAM levels were evaluated by Western Blot analysis, 48h following transfections or in stably transduced cells. Protein

modulations were calculated relative to negative controls, normalized on loading controls (GAPDH or Actin) and expressed as percentages (%). Transmigration results are indicated as mean±SEM of the area covered by migrated cells. At least 2 independent experiments (with triplicates) were performed and representative results are shown. SEM= Standard Error of Mean. (C-D) *In vivo* extravasation 2h or 48h following tail vein injections in immunocompromised mice of CMRA-labeled MA-2 cells transfected with si-control or si-ITGA5 or transduced for sh-ALCAM or sh-control, as indicated. Representative pictures of whole red fluorescent lungs are shown (a-b=2h; c-d=48h); bar=800 μm. Results are indicated as mean±SEM of the number of extravasated cells at 48 h for n=4 mice per group. 2 independent experiments were carried out (with triplicates) and representative ones are shown. SEM= Standard Error of Mean. (E) Confocal microscopy image for HUVECs-MA-2 co-cultures: HUVECs are green for GFP expression, MA-2 are red for ALCAM staining. Nuclei are blue for DAPI staining.

A MC-1

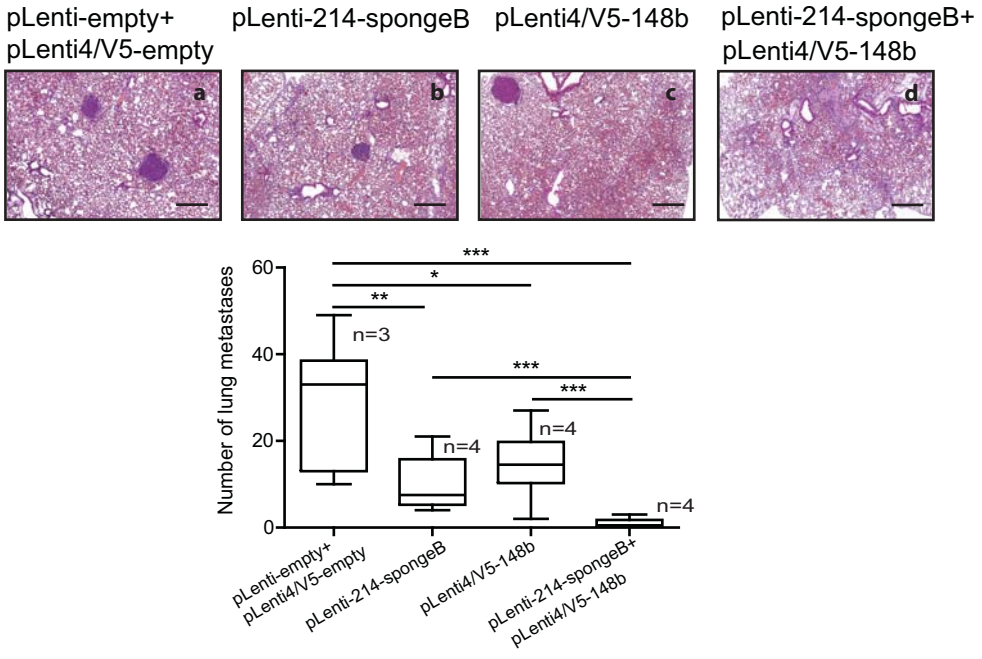

B 4175-TGL

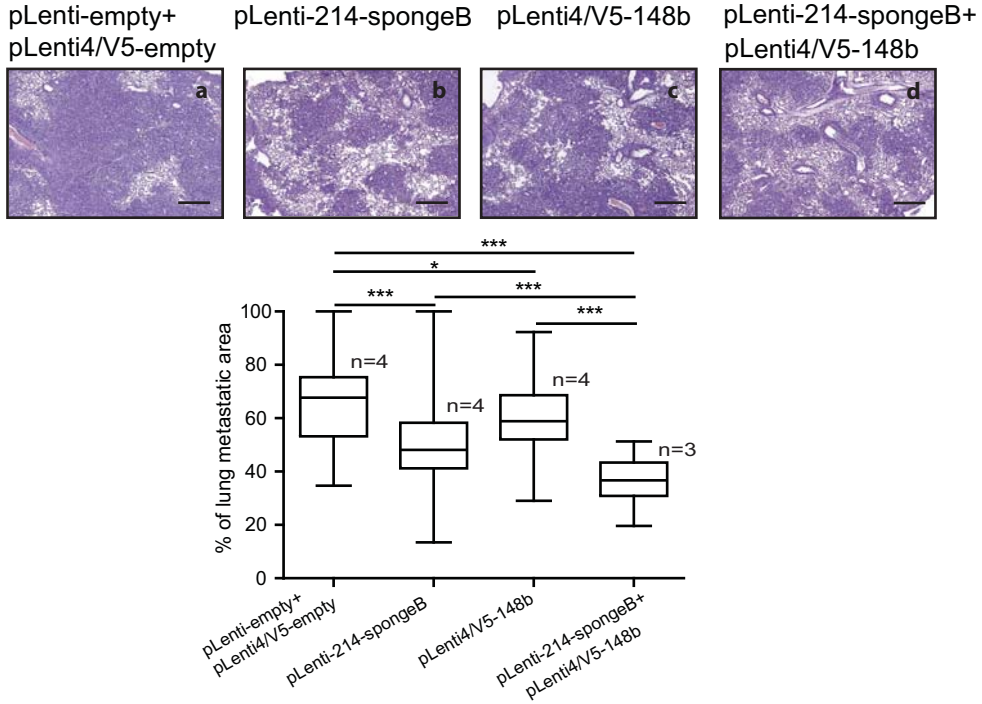

C 4175-TGL

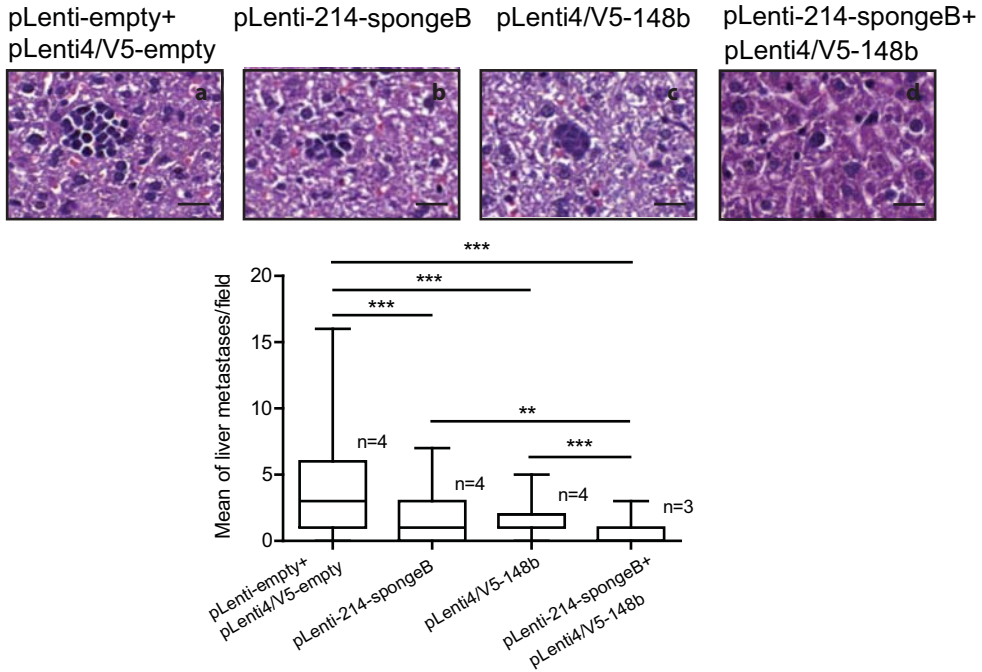

A

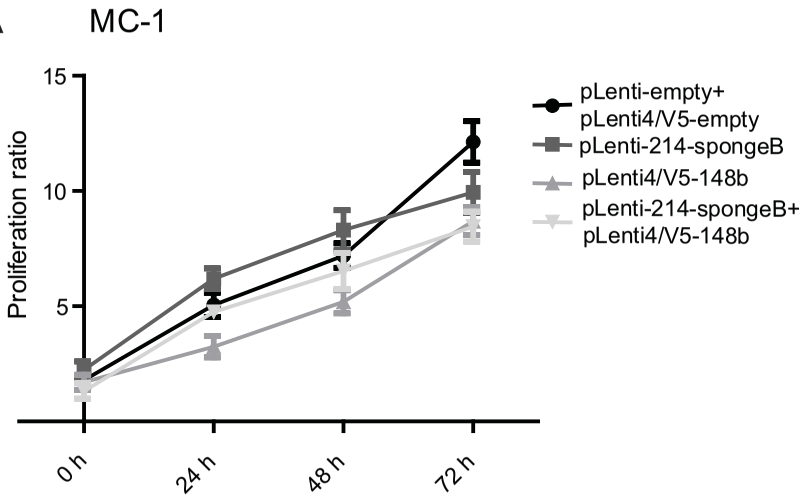
MC-1
Proliferation ratio
15
10
5
0 h
24 h
48 h
72 h
pLenti-empty+
pLenti4/V5-empty
pLenti-214-spongeB
pLenti4/V5-148b
pLenti-214-spongeB+
pLenti4/V5-148b

B

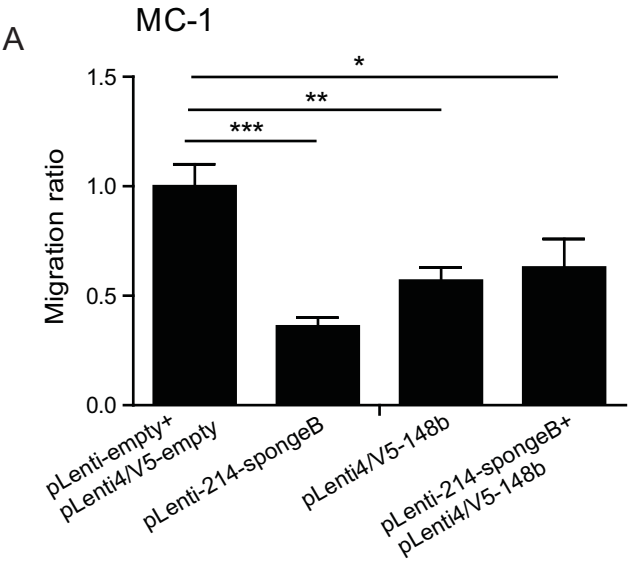
A
MC-1
Migration ratio
1.5
1.0
0.5
0.0
*
**
***
pLenti-empty+ pLenti4/V5-empty
pLenti-214-spongeB
pLenti4/V5-148b
pLenti-214-spongeB+ pLenti4/V5-148b

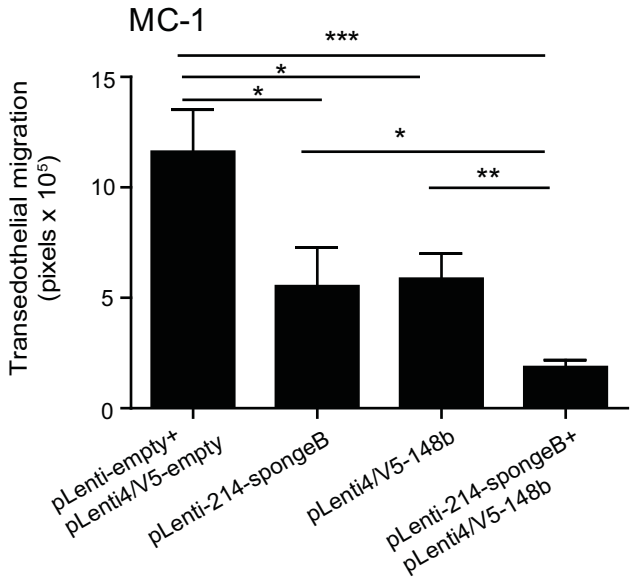
B
MC-1
Transedothelial migration (pixels x 10⁵)
15
10
5
0
***
*
*
*
**
pLenti-empty+ pLenti4/V5-empty
pLenti-214-spongeB
pLenti4/V5-148b
pLenti-214-spongeB+ pLenti4/V5-148b

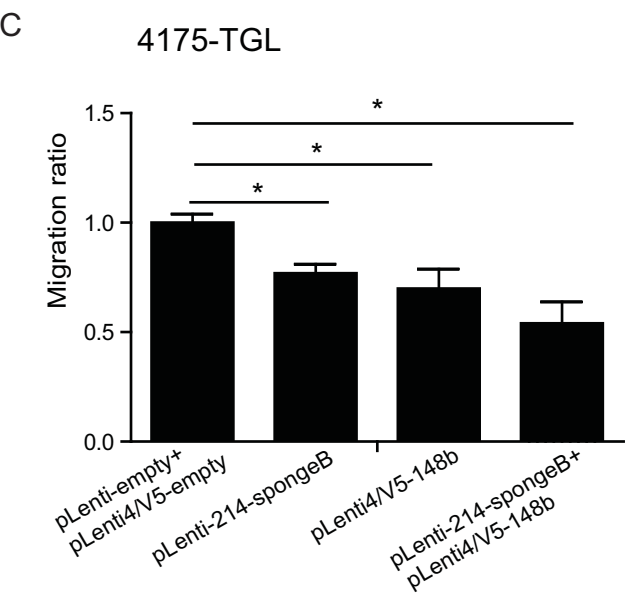
C
4175-TGL
Migration ratio
1.5
1.0
0.5
0.0
*
*
*
pLenti-empty+ pLenti4/V5-empty
pLenti-214-spongeB
pLenti4/V5-148b
pLenti-214-spongeB+ pLenti4/V5-148b

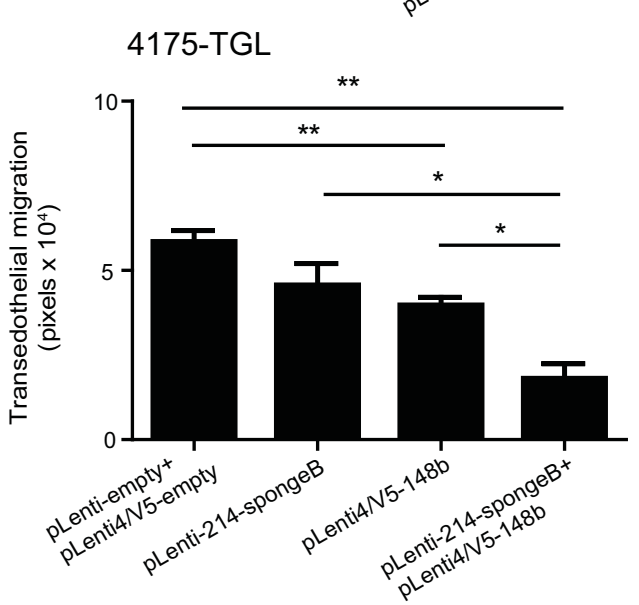
D
4175-TGL
Transedothelial migration (pixels x 10⁴)
10
5
0
**
**
*
*
pLenti-empty+ pLenti4/V5-empty
pLenti-214-spongeB
pLenti4/V5-148b
pLenti-214-spongeB+ pLenti4/V5-148b

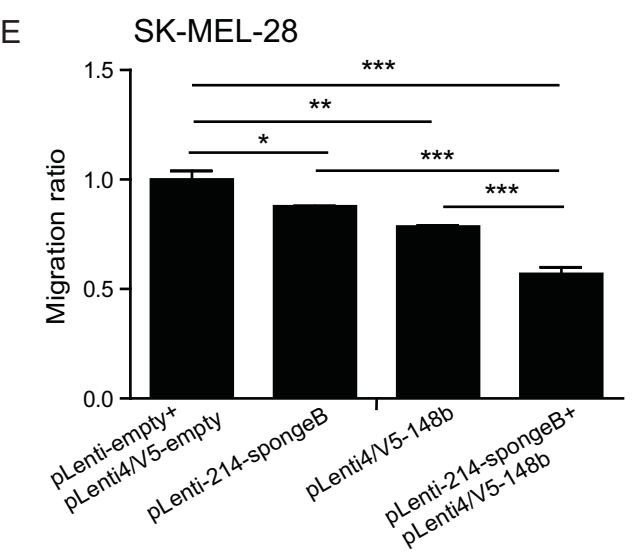
E
SK-MEL-28
Migration ratio
1.5
1.0
0.5
0.0
***
**
*
***
***
pLenti-empty+ pLenti4/V5-empty
pLenti-214-spongeB
pLenti4/V5-148b
pLenti-214-spongeB+ pLenti4/V5-148b

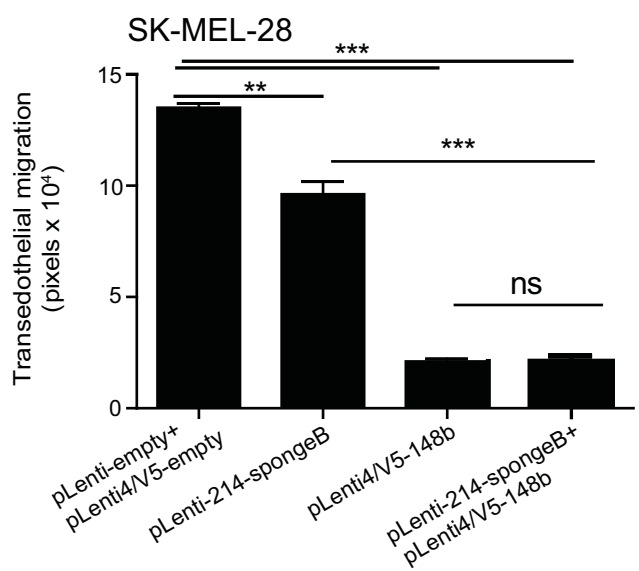
F
SK-MEL-28
Transedothelial migration (pixels x 10⁴)
15
10
5
0
***
**
***
ns
pLenti-empty+ pLenti4/V5-empty
pLenti-214-spongeB
pLenti4/V5-148b
pLenti-214-spongeB+ pLenti4/V5-148b

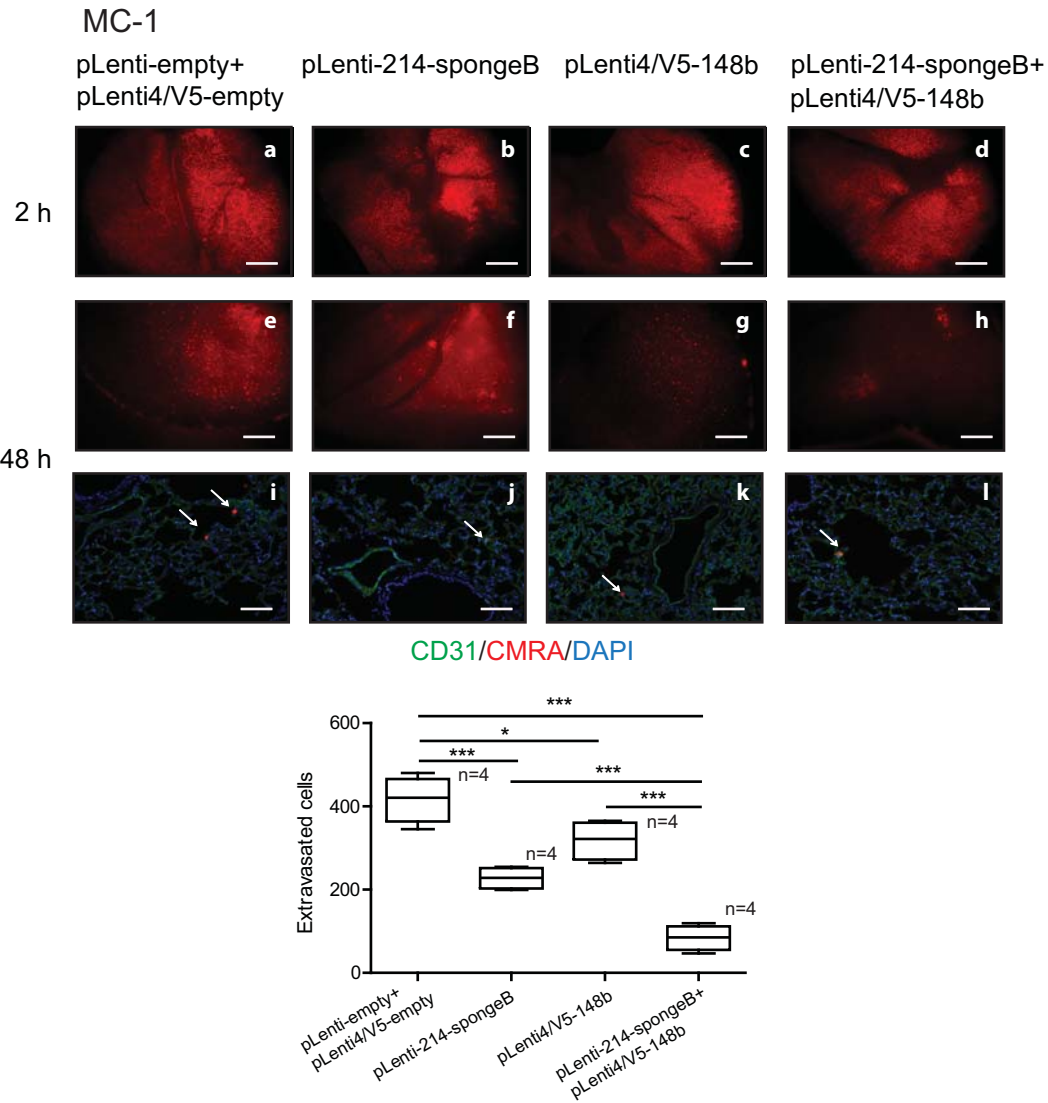
MC-1
pLenti-empty+ pLenti4/V5-empty
pLenti-214-spongeB
pLenti4/V5-148b
pLenti-214-spongeB+ pLenti4/V5-148b
2 h
48 h
a
b
c
d
e
f
g
h
i
j
k
l
CD31/CMRA/DAPI
Extravasated cells
600
400
200
0
***
*
***
***
***
n=4
n=4
n=4
n=4
pLenti-empty+ pLenti4/V5-empty
pLenti-214-spongeB
pLenti4/V5-148b
pLenti-214-spongeB+ pLenti4/V5-148b

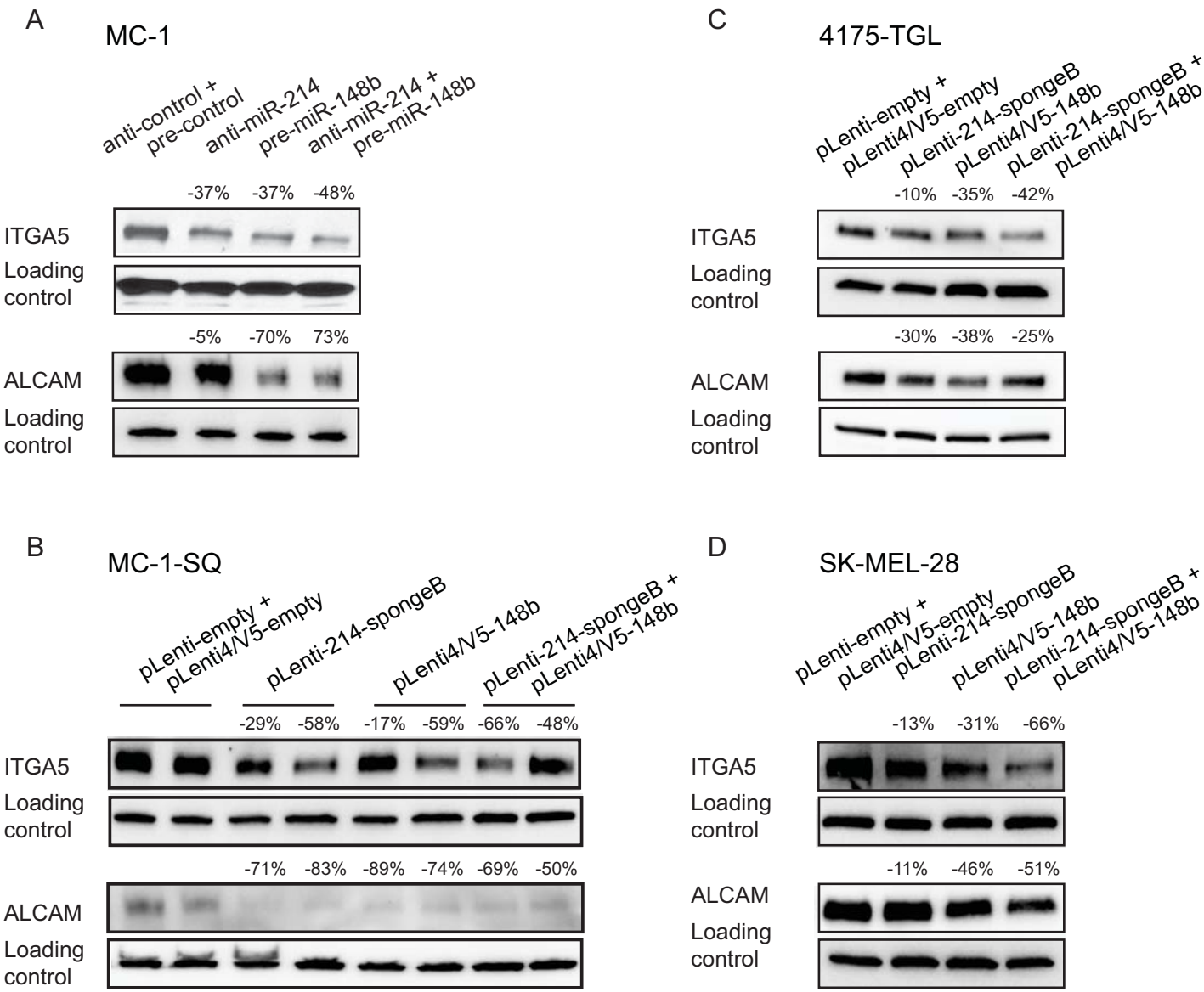
A
MC-1
anti-control + pre-control
anti-miR-214
pre-miR-148b
anti-miR-214 + pre-miR-148b
-37% -37% -48%
ITGA5
Loading control
-5% -70% 73%
ALCAM
Loading control
C
4175-TGL
pLenti-empty + pLenti4/V5-empty
pLenti-214-spongeB
pLenti4/V5-148b
pLenti-214-spongeB + pLenti4/V5-148b
-10% -35% -42%
ITGA5
Loading control
-30% -38% -25%
ALCAM
Loading control
B
MC-1-SQ
pLenti-empty + pLenti4/V5-empty
pLenti-214-spongeB
pLenti4/V5-148b
pLenti-214-spongeB + pLenti4/V5-148b
-29% -58% -17% -59% -66% -48%
ITGA5
Loading control
-71% -83% -89% -74% -69% -50%
ALCAM
Loading control
D
SK-MEL-28
pLenti-empty + pLenti4/V5-empty
pLenti-214-spongeB
pLenti4/V5-148b
pLenti-214-spongeB + pLenti4/V5-148b
-13% -31% -66%
ITGA5
Loading control
-11% -46% -51%
ALCAM
Loading control

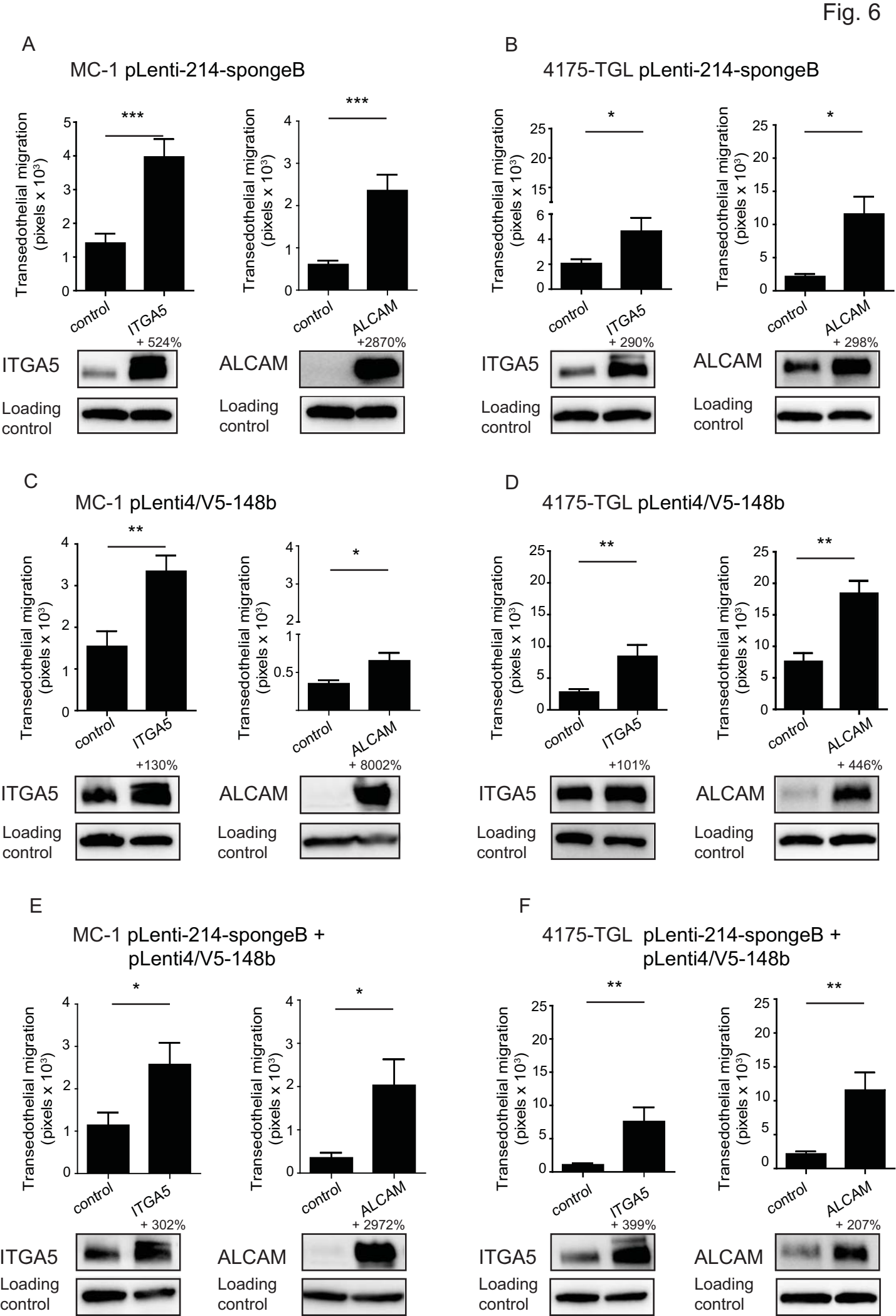
A
MC-1 pLenti-214-spongeB
Transedothelial migration (pixels x 10³)
***
control
ITGA5
+ 524%
ITGA5
Loading control
***
control
ALCAM
+2870%
ALCAM
Loading control
B
4175-TGL pLenti-214-spongeB
*
control
ITGA5
+ 290%
ITGA5
Loading control
*
control
ALCAM
+ 298%
ALCAM
Loading control
C
MC-1 pLenti4/V5-148b
**
control
ITGA5
+130%
ITGA5
Loading control
*
control
ALCAM
+ 8002%
ALCAM
Loading control
D
4175-TGL pLenti4/V5-148b
**
control
ITGA5
+101%
ITGA5
Loading control
**
control
ALCAM
+ 446%
ALCAM
Loading control
E
MC-1 pLenti-214-spongeB + pLenti4/V5-148b
*
control
ITGA5
+ 302%
ITGA5
Loading control
*
control
ALCAM
+ 2972%
ALCAM
Loading control
F
4175-TGL pLenti-214-spongeB + pLenti4/V5-148b
**
control
ITGA5
+ 399%
ITGA5
Loading control
**
control
ALCAM
+ 207%
ALCAM
Loading control

A

Melanoma Dataset
(TGCA)
Metastases

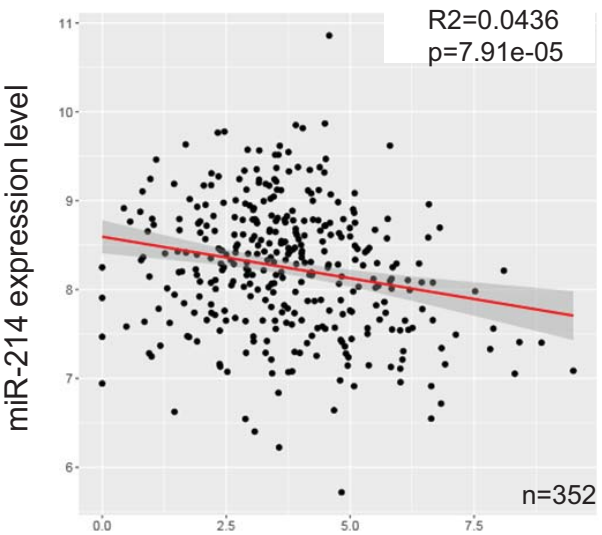

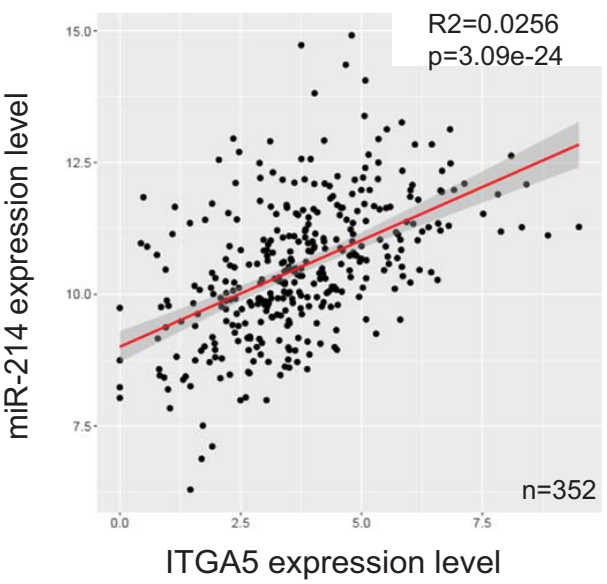

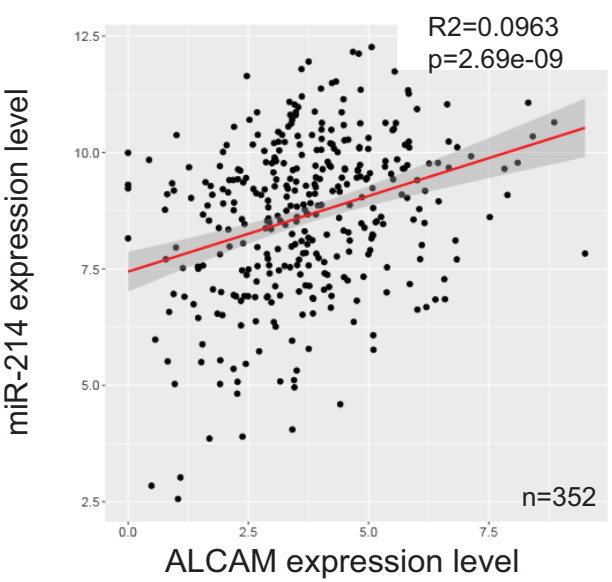

B

Breast Cancer Dataset
(Dvinge et al., 2013; Curtis et al., 2012)
Primary

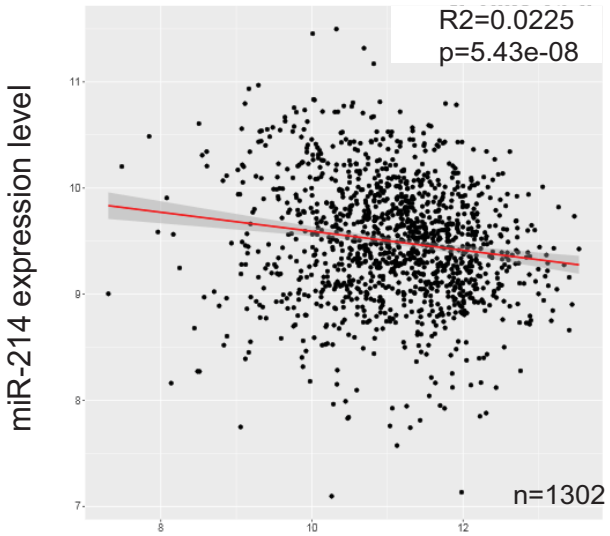

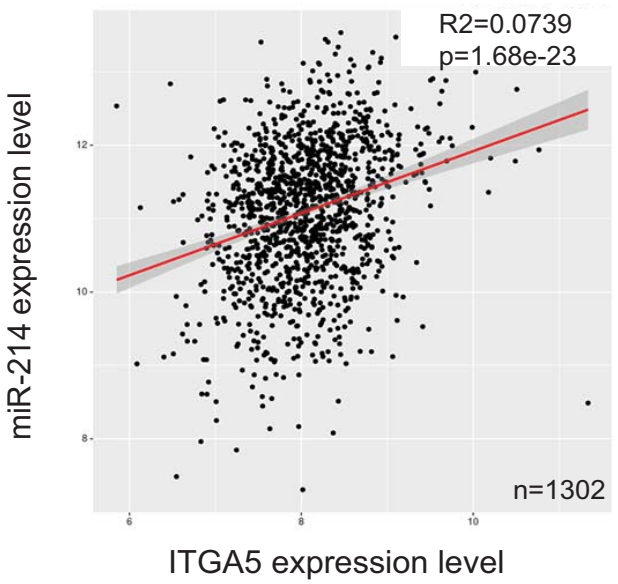

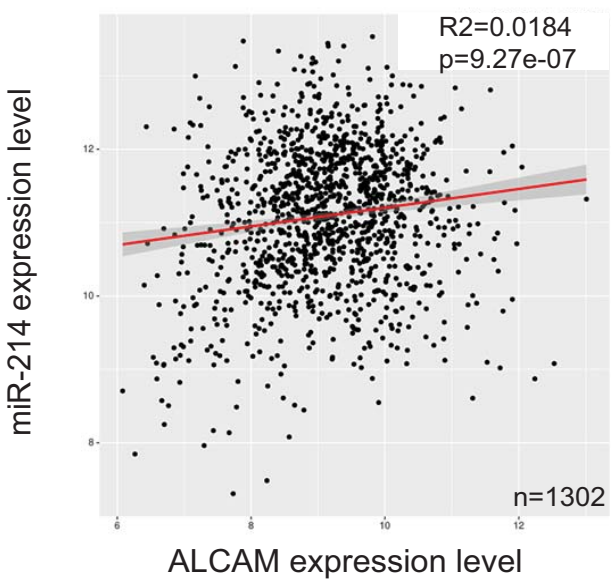

miRNA sponge	Sequence	length	n° of sites
214-spongeA	TTGAAGCTTACTGCCTGTCAATCCTGCTGTCTAAACATAATTCCTACTGCCTGTC CATCCTGCTGTCCTTTCTATTCCCTCACTGCCTGTCCATCCTGCTGTCCCATTGA AATATATACTGCCTGTCTACCCTGCTGTCATTAAAACGCCCCTACTGCCTGTCCC TCCTGCTGTCAAACCTAACTTACAACTGCCTGTCCCCCCTGCTGTCCACTGAAAC TTCCTACTGCCTGTCTCTCCTGCTGTCCTCAAATTTACCTAACTGCCTGTCCCCC CTGCTGTGCAAGCTTGC	292 bp	8
214-spongeB	TTGAAGCTTACTGCCTGTCTATCCTGCTGTCATCTTTATATCTAAACTGCCTGTCA ACCCTGCTGTCACCTCCTAACAAAAACTGCCTGTCTCTCCTGCTGTCACATCACT CCCGCCACTGCCTGTCCCCCCTGCTGTCACCATATCCTACACACTGCCTGTCTC CCCTGCTGTCTTAACTACATATATACTGCCTGTCCCCCCTGCTGTCTACAAATAC CCCCTACTGCCTGTCTCCCCTGCTGTCCAACATTTCCAATCACTGCCTGTCACTC CTGCTGTGCAAGCTTGC	292 bp	8
148b-spongeA	TTGAAGCTTACAAAGTTCTGCCTGCACTGAAACCTAAACCTACCTACAAAGTTCT GACTGCACTGATTTCCACAATAAAAAACAAAGTTCTGCGTGCACTGATTAAAATTT CCATATACAAAGTTCTGCCTGCACTGACATCTCATAACCTGGACAAAGTTCTGCC TGCACTGATAAAAAAGACATAATACAAAGTTCTCCCTGCACTGAGTTCCCCACCA CACCACAAAGTTCTACTTGCACTGAATCCACCACCCAATAACAAAGTTCTATCTG CACTGAGCAAGCTTGC	292 bp	8
148b-spongeB	TTGAAGCTTACAAAGTTCTCTGTGCACTGACATTACCCCCTCTACACAAAGTTCT CCCTGCACTGACCATAAACCTACACCACAAAGTTCTGATTGCACTGATTCCCCTC TCTATTAACAAAGTTCTACCTGCACTGACCATCCACCCAATTTACAAAGTTCTGC CTGCACTGAAAAATATCTATCTCCACAAAGTTCTGCCTGCACTGATCTCATACAA AATATACAAAGTTCTGACTGCACTGATAATAATACCACCCTACAAAGTTCTAACTG CACTGAGCAAGCTTGC	292 bp	8

Penna, Orso et al., EMBO J, 2011

Fig. S1

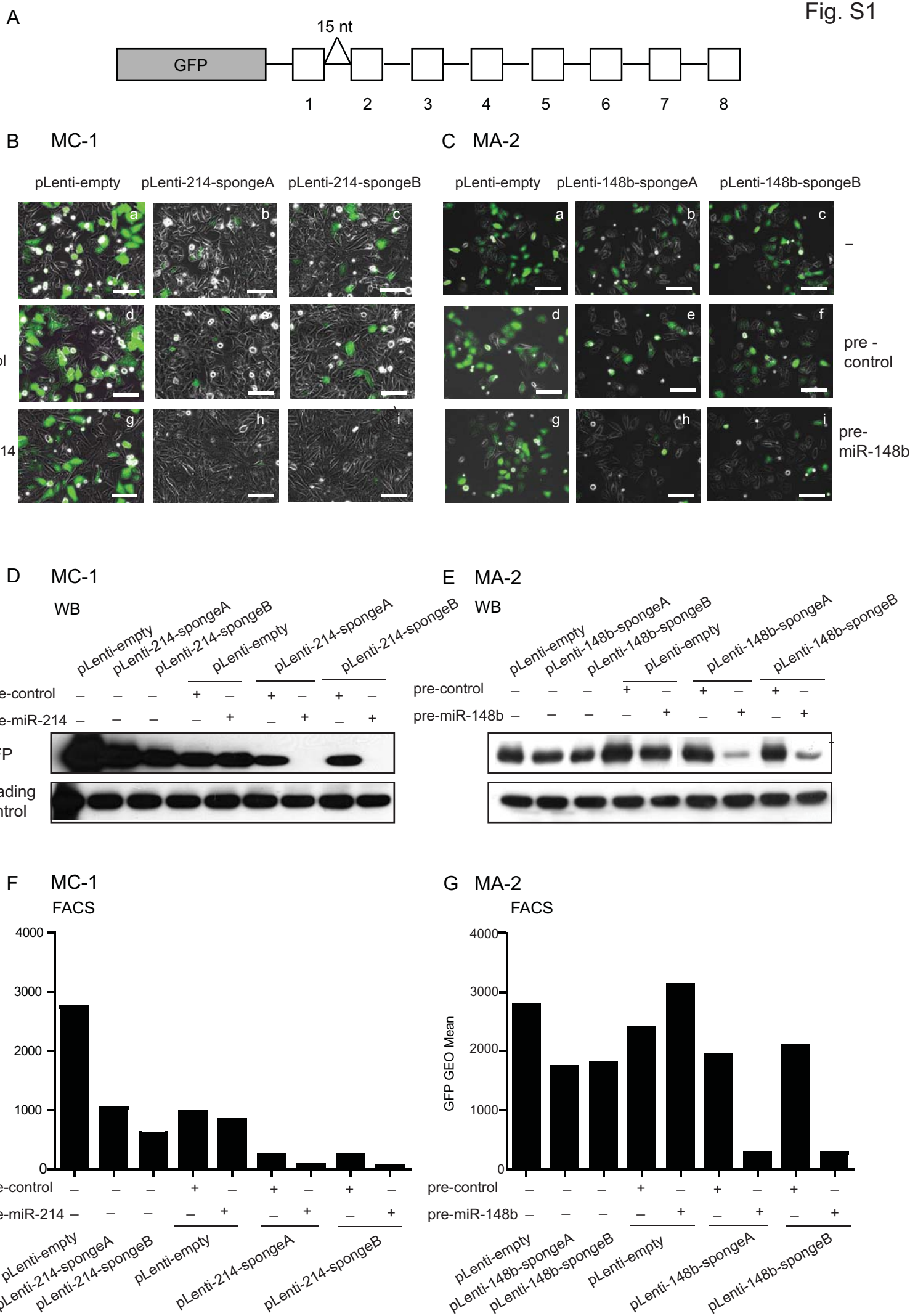
A
15 nt
GFP
1
2
3
4
5
6
7
8
B MC-1
pLenti-empty
pLenti-214-spongeA
pLenti-214-spongeB
–
pre-control
pre-miR-214
C MA-2
pLenti-empty
pLenti-148b-spongeA
pLenti-148b-spongeB
–
pre - control
pre-miR-148b
D MC-1
WB
pLenti-empty
pLenti-214-spongeA
pLenti-214-spongeB
pLenti-empty
pLenti-214-spongeA
pLenti-214-spongeB
pre-control
pre-miR-214
GFP
Loading control
E MA-2
WB
pLenti-empty
pLenti-148b-spongeA
pLenti-148b-spongeB
pLenti-empty
pLenti-148b-spongeA
pLenti-148b-spongeB
pre-control
pre-miR-148b
F MC-1
FACS
GFP GEO Mean
4000
3000
2000
1000
0
pre-control
pre-miR-214
pLenti-empty
pLenti-214-spongeA
pLenti-214-spongeB
pLenti-empty
pLenti-214-spongeA
pLenti-214-spongeB
G MA-2
FACS
GFP GEO Mean
4000
3000
2000
1000
0
pre-control
pre-miR-148b
pLenti-empty
pLenti-148b-spongeA
pLenti-148b-spongeB
pLenti-empty
pLenti-148b-spongeA
pLenti-148b-spongeB

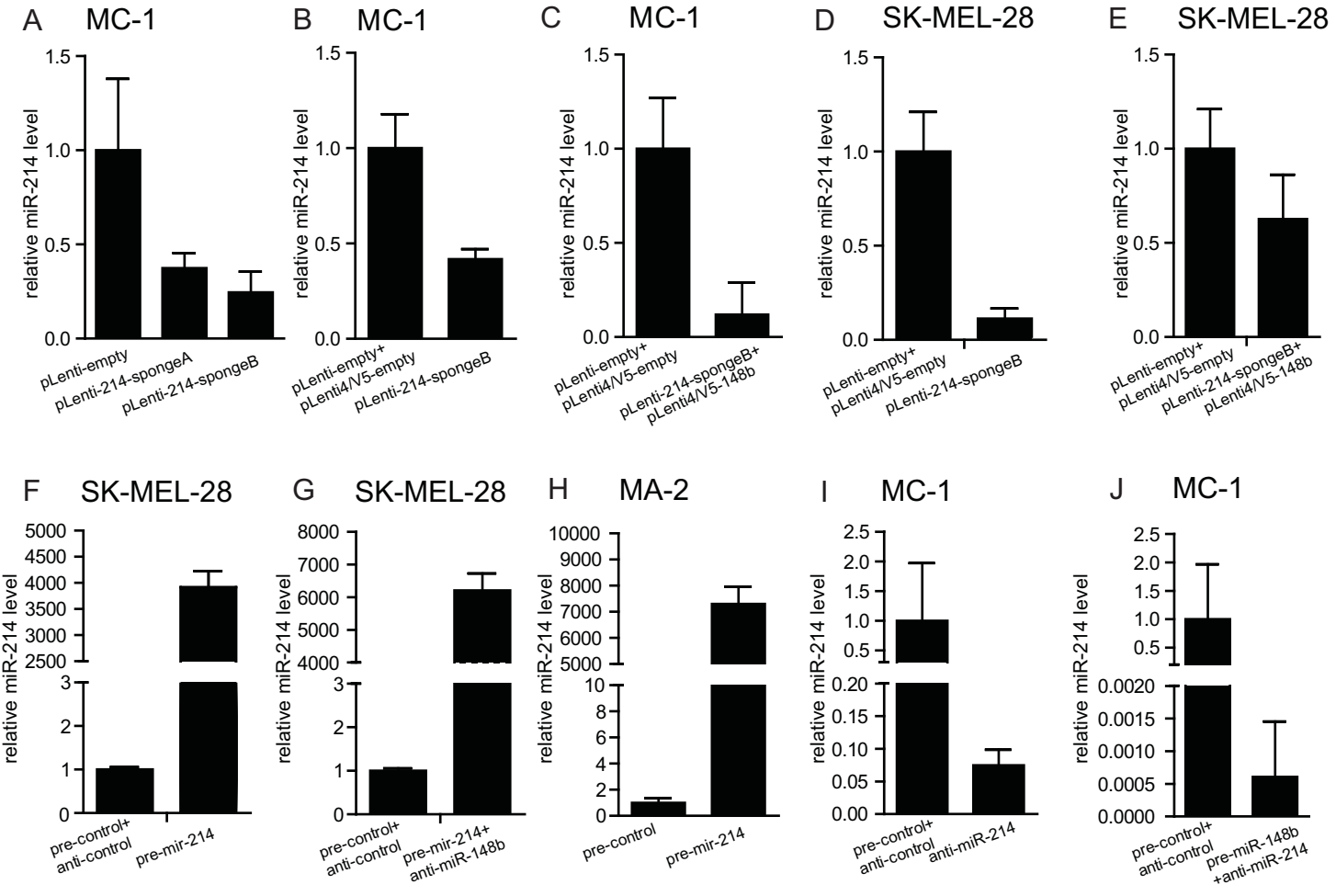
A
MC-1
relative miR-214 level
1.5
1.0
0.5
0.0
pLenti-empty
pLenti-214-spongeA
pLenti-214-spongeB
B
MC-1
relative miR-214 level
1.5
1.0
0.5
0.0
pLenti-empty+
pLenti4/V5-empty
pLenti-214-spongeB
C
MC-1
relative miR-214 level
1.5
1.0
0.5
0.0
pLenti-empty+
pLenti4/V5-empty
pLenti-214-spongeB+
pLenti4/V5-148b
D
SK-MEL-28
relative miR-214 level
1.5
1.0
0.5
0.0
pLenti-empty+
pLenti4/V5-empty
pLenti-214-spongeB
E
SK-MEL-28
relative miR-214 level
1.5
1.0
0.5
0.0
pLenti-empty+
pLenti4/V5-empty
pLenti-214-spongeB+
pLenti4/V5-148b
F
SK-MEL-28
relative miR-214 level
5000
4500
4000
3500
3000
2500
3
2
1
0
pre-control+
anti-control
pre-mir-214
G
SK-MEL-28
relative miR-214 level
8000
7000
6000
5000
4000
3
2
1
0
pre-control+
anti-control
pre-mir-214+
anti-miR-148b
H
MA-2
relative miR-214 level
10000
9000
8000
7000
6000
5000
10
8
6
4
2
0
pre-control
pre-mir-214
I
MC-1
relative miR-214 level
2.5
2.0
1.5
1.0
0.5
0.20
0.15
0.10
0.05
0.00
pre-control+
anti-control
anti-miR-214
J
MC-1
relative miR-214 level
2.5
2.0
1.5
1.0
0.5
0.0020
0.0015
0.0010
0.0005
0.0000
pre-control+
anti-control
pre-miR-148b
+anti-miR-214

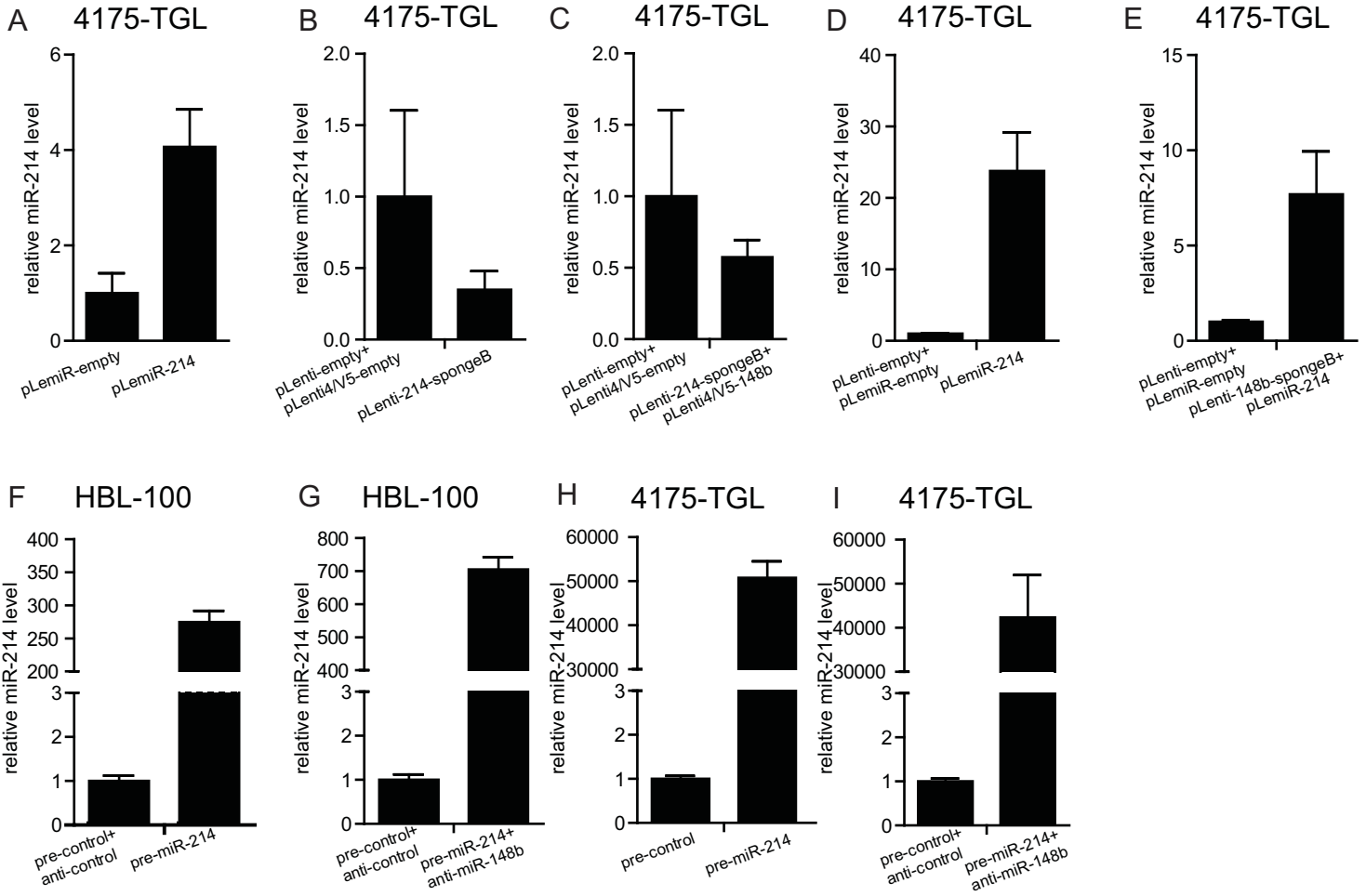
A
4175-TGL
relative miR-214 level
pLemiR-empty
pLemiR-214
B
4175-TGL
relative miR-214 level
pLenti-empty+ pLenti4/V5-empty
pLenti-214-spongeB
C
4175-TGL
relative miR-214 level
pLenti-empty+ pLenti4/V5-empty
pLenti-214-spongeB+ pLenti4/V5-148b
D
4175-TGL
relative miR-214 level
pLenti-empty+ pLemiR-empty
pLemiR-214
E
4175-TGL
relative miR-214 level
pLenti-empty+ pLemiR-empty
pLenti-148b-spongeB+ pLemiR-214
F
HBL-100
relative miR-214 level
pre-control+ anti-control
pre-miR-214
G
HBL-100
relative miR-214 level
pre-control+ anti-control
pre-miR-214+ anti-miR-148b
H
4175-TGL
relative miR-214 level
pre-control
pre-miR-214
I
4175-TGL
relative miR-214 level
pre-control+ anti-control
pre-miR-214+ anti-miR-148b

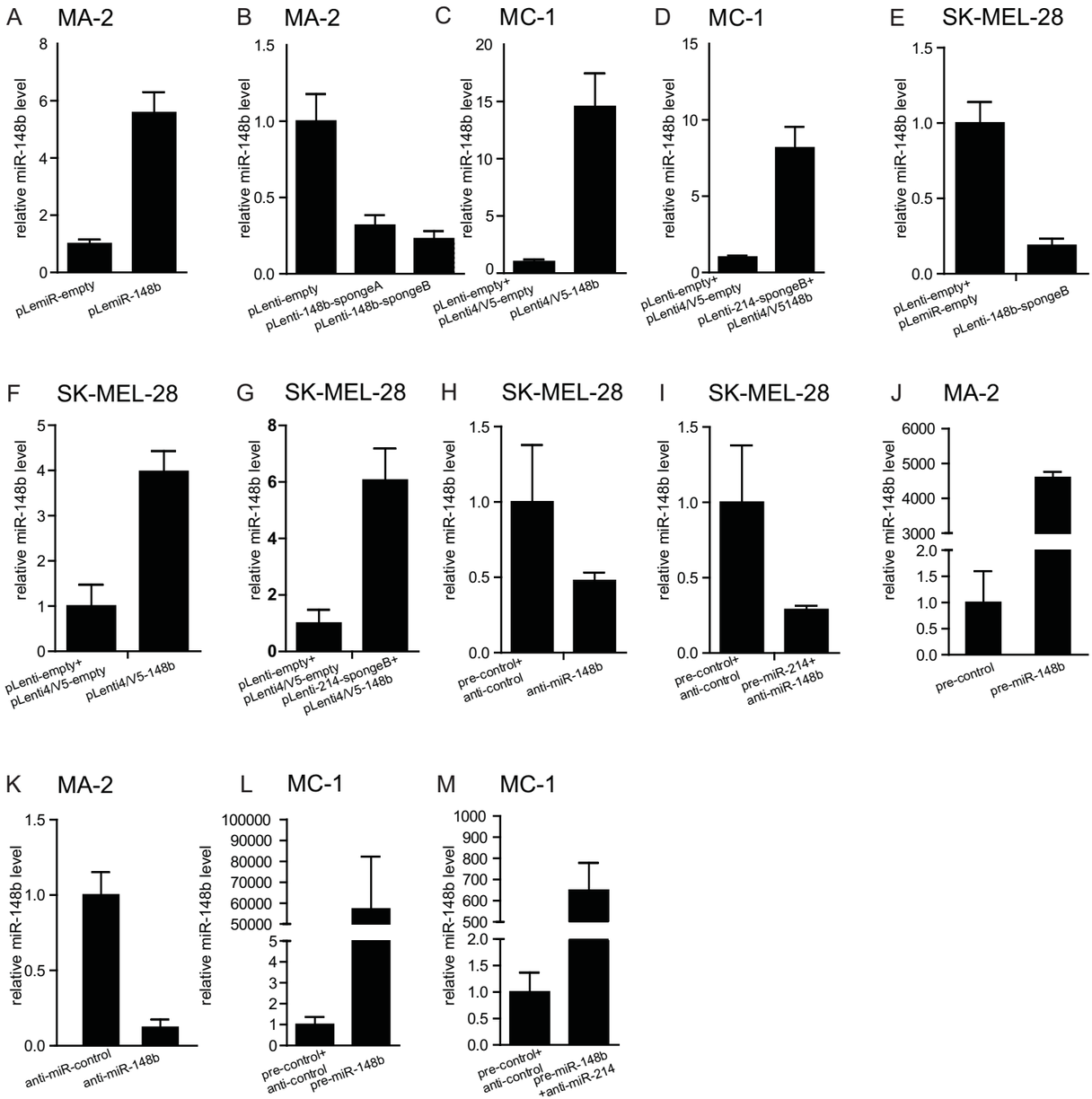
A MA-2
relative miR-148b level
pLemiR-empty
pLemiR-148b
B MA-2
relative miR-148b level
pLenti-empty
pLenti-148b-spongeA
pLenti-148b-spongeB
C MC-1
relative miR-148b level
pLenti-empty+ pLenti4/V5-empty
pLenti4/V5-148b
D MC-1
relative miR-148b level
pLenti-empty+ pLenti4/V5-empty
pLenti-214-spongeB+ pLenti4/V5148b
E SK-MEL-28
relative miR-148b level
pLenti-empty+ pLemiR-empty
pLenti-148b-spongeB
F SK-MEL-28
relative miR-148b level
pLenti-empty+ pLenti4/V5-empty
pLenti4/V5-148b
G SK-MEL-28
relative miR-148b level
pLenti-empty+ pLenti4/V5-empty
pLenti-214-spongeB+ pLenti4/V5-148b
H SK-MEL-28
relative miR-148b level
pre-control+ anti-control
anti-miR-148b
I SK-MEL-28
relative miR-148b level
pre-control+ anti-control
pre-miR-214+ anti-miR-148b
J MA-2
relative miR-148b level
pre-control
pre-miR-148b
K MA-2
relative miR-148b level
anti-miR-control
anti-miR-148b
L MC-1
relative miR-148b level
pre-control+ anti-control
pre-miR-148b
M MC-1
relative miR-148b level
pre-control+ anti-control
pre-miR-148b +anti-miR-214

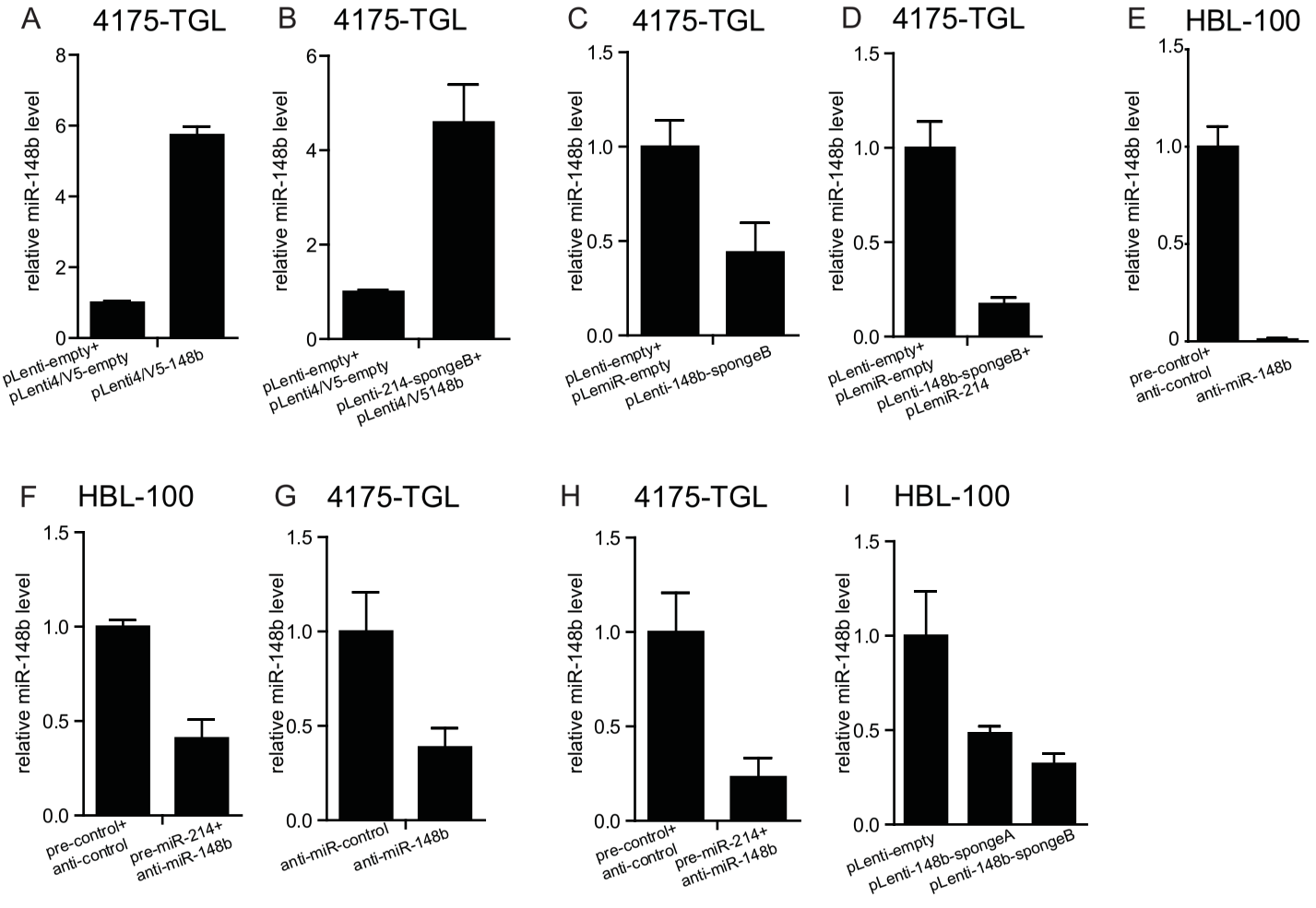
A
4175-TGL
relative miR-148b level
8
6
4
2
0
pLenti-empty+
pLenti4/V5-empty
pLenti4/V5-148b
B
4175-TGL
relative miR-148b level
6
4
2
0
pLenti-empty+
pLenti4/V5-empty
pLenti-214-spongeB+
pLenti4/V5148b
C
4175-TGL
relative miR-148b level
1.5
1.0
0.5
0.0
pLenti-empty+
pLemiR-empty
pLenti-148b-spongeB
D
4175-TGL
relative miR-148b level
1.5
1.0
0.5
0.0
pLenti-empty+
pLemiR-empty
pLenti-148b-spongeB+
pLemiR-214
E
HBL-100
relative miR-148b level
1.5
1.0
0.5
0
pre-control+
anti-control
anti-miR-148b
F
HBL-100
relative miR-148b level
1.5
1.0
0.5
0.0
pre-control+
anti-control
pre-miR-214+
anti-miR-148b
G
4175-TGL
relative miR-148b level
1.5
1.0
0.5
0.0
anti-miR-control
anti-miR-148b
H
4175-TGL
relative miR-148b level
1.5
1.0
0.5
0.0
pre-control+
anti-control
pre-miR-214+
anti-miR-148b
I
HBL-100
relative miR-148b level
1.5
1.0
0.5
0.0
pLenti-empty
pLenti-148b-spongeA
pLenti-148b-spongeB

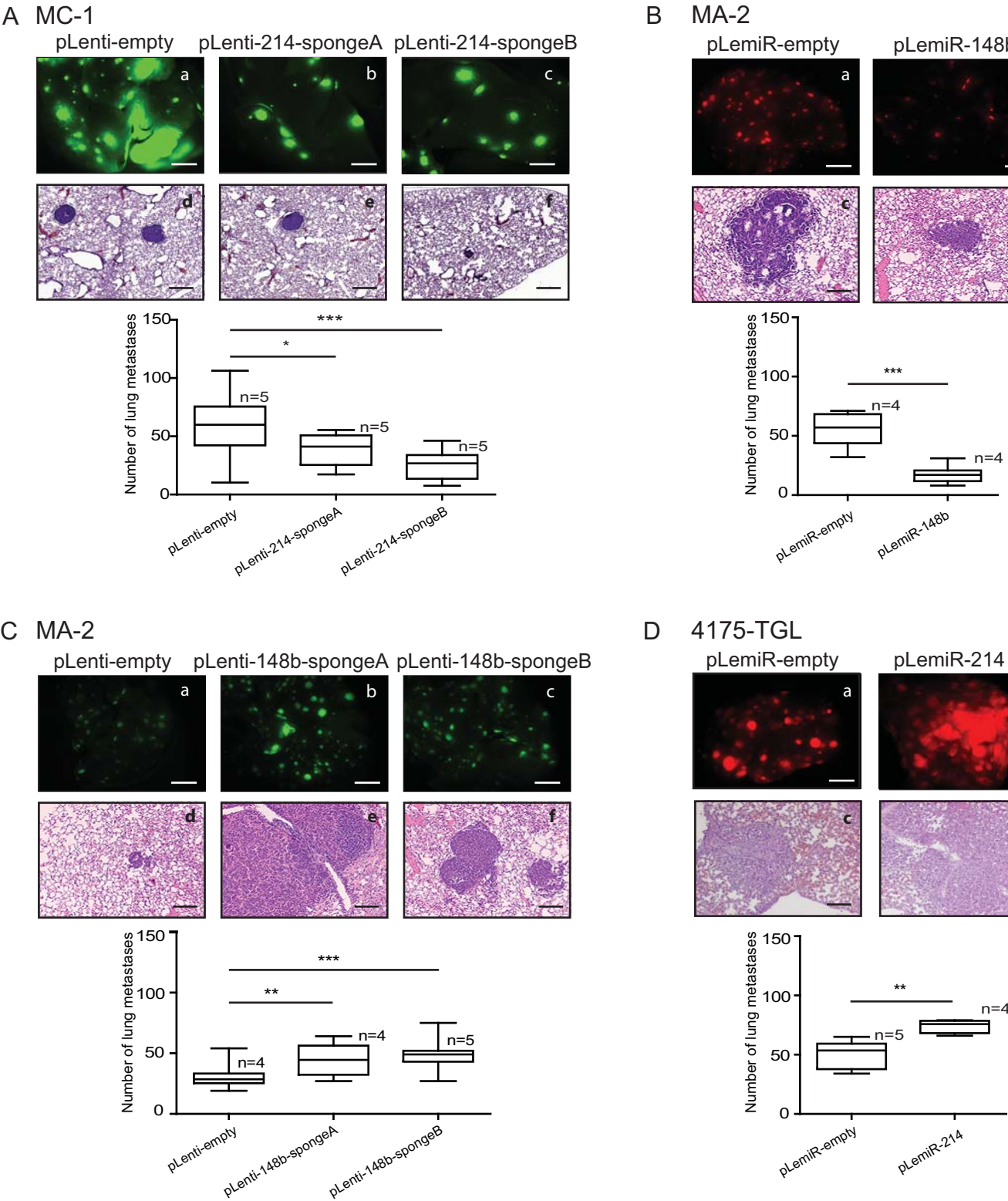
A MC-1
pLenti-empty
pLenti-214-spongeA
pLenti-214-spongeB
a
b
c
d
e
f
Number of lung metastases
150
100
50
0
***
*
n=5
n=5
n=5
pLenti-empty
pLenti-214-spongeA
pLenti-214-spongeB
B MA-2
pLemiR-empty
pLemiR-148b
a
b
c
d
Number of lung metastases
150
100
50
0
***
n=4
n=4
pLemiR-empty
pLemiR-148b
C MA-2
pLenti-empty
pLenti-148b-spongeA
pLenti-148b-spongeB
a
b
c
d
e
f
Number of lung metastases
150
100
50
0
***
**
n=4
n=4
n=5
pLenti-empty
pLenti-148b-spongeA
pLenti-148b-spongeB
D 4175-TGL
pLemiR-empty
pLemiR-214
a
b
c
d
Number of lung metastases
150
100
50
0
**
n=5
n=4
pLemiR-empty
pLemiR-214

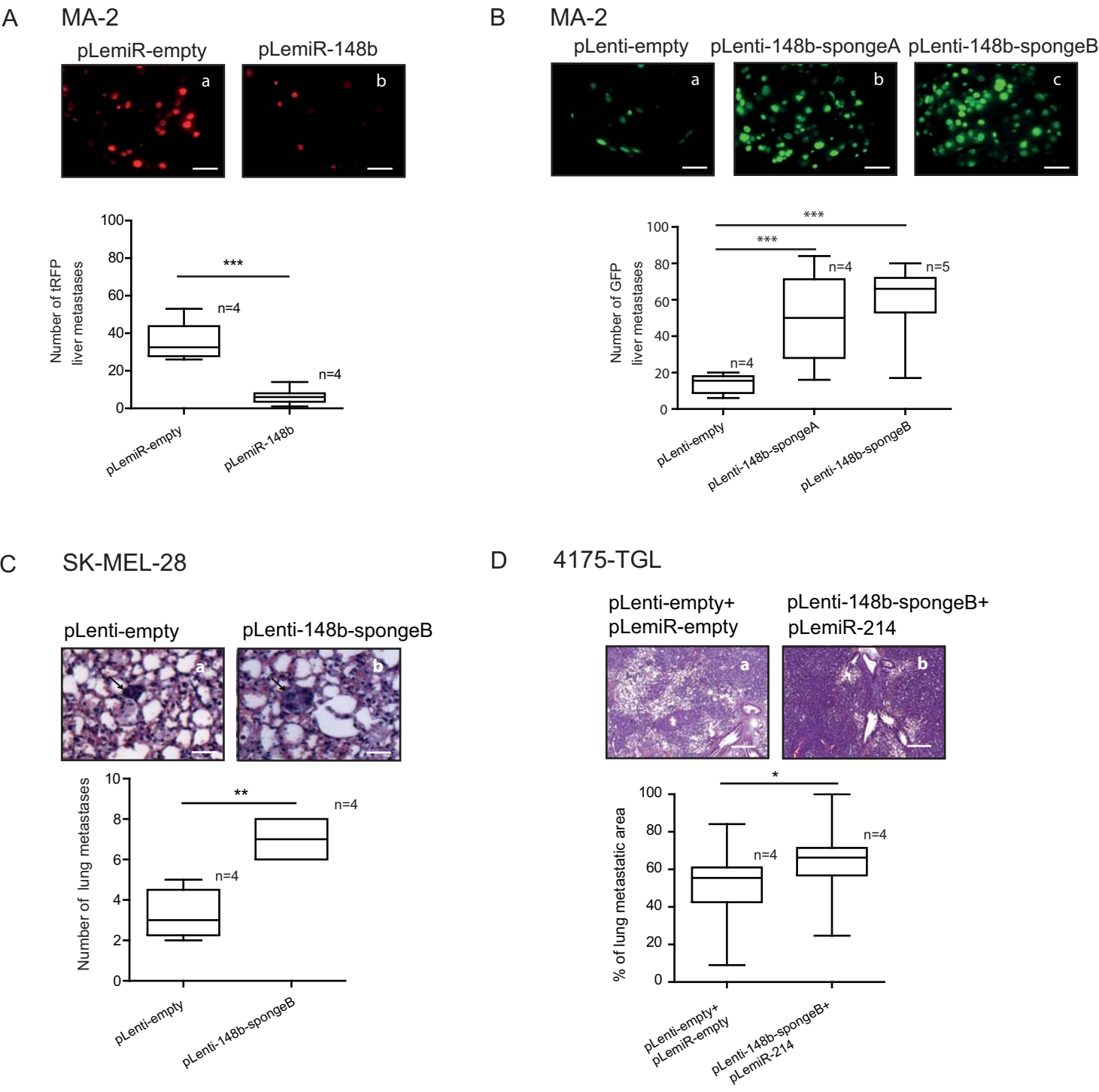
A
MA-2
pLemiR-empty
pLemiR-148b
a
b
Number of tRFP liver metastases
***
n=4
n=4
pLemiR-empty
pLemiR-148b
B
MA-2
pLenti-empty
pLenti-148b-spongeA
pLenti-148b-spongeB
a
b
c
Number of GFP liver metastases
***
***
n=4
n=4
n=5
pLenti-empty
pLenti-148b-spongeA
pLenti-148b-spongeB
C
SK-MEL-28
pLenti-empty
pLenti-148b-spongeB
a
b
Number of lung metastases
**
n=4
n=4
pLenti-empty
pLenti-148b-spongeB
D
4175-TGL
pLenti-empty+
pLemiR-empty
pLenti-148b-spongeB+
pLemiR-214
a
b
% of lung metastatic area
*
n=4
n=4
pLenti-empty+
pLemiR-empty
pLenti-148b-spongeB+
pLemiR-214

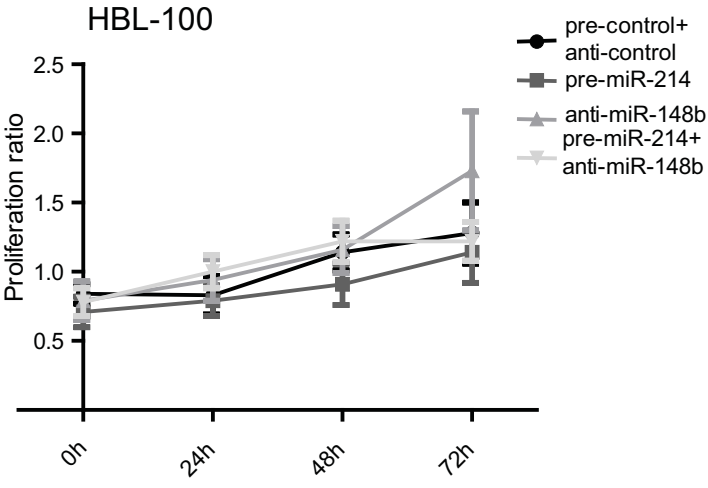
HBL-100
Proliferation ratio
2.5
2.0
1.5
1.0
0.5
0h
24h
48h
72h
pre-control+
anti-control
pre-miR-214
anti-miR-148b
pre-miR-214+
anti-miR-148b

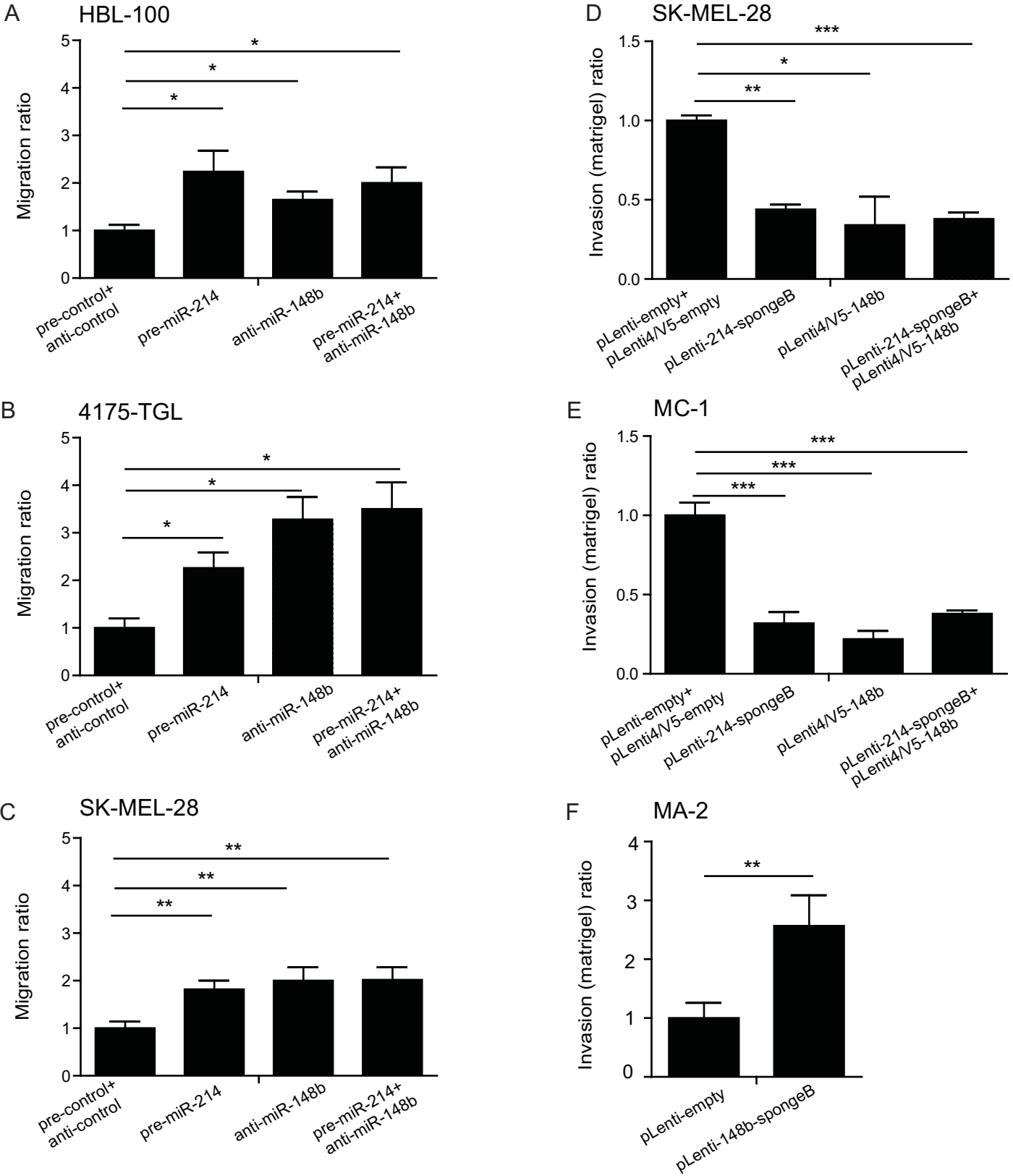
A
HBL-100
Migration ratio
pre-control+ anti-control
pre-miR-214
anti-miR-148b
pre-miR-214+ anti-miR-148b
B
4175-TGL
Migration ratio
C
SK-MEL-28
Migration ratio
D
SK-MEL-28
Invasion (matrigel) ratio
pLenti-empty+ pLenti4/V5-empty
pLenti-214-spongeB
pLenti4/V5-148b
pLenti-214-spongeB+ pLenti4/V5-148b
E
MC-1
Invasion (matrigel) ratio
F
MA-2
Invasion (matrigel) ratio
pLenti-empty
pLenti-148b-spongeB

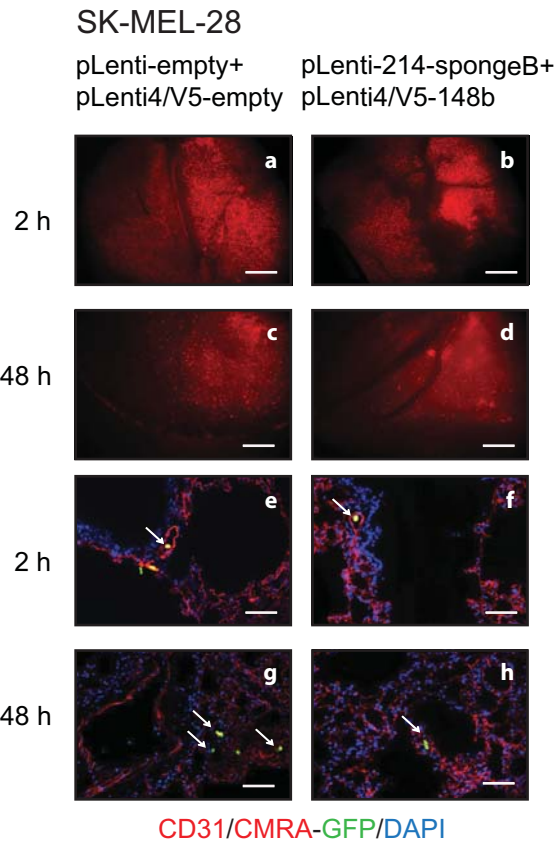
SK-MEL-28
pLenti-empty+
pLenti4/V5-empty
pLenti-214-spongeB+
pLenti4/V5-148b
2 h
48 h
2 h
48 h
a
b
c
d
e
f
g
h
CD31/CMRA-GFP/DAPI

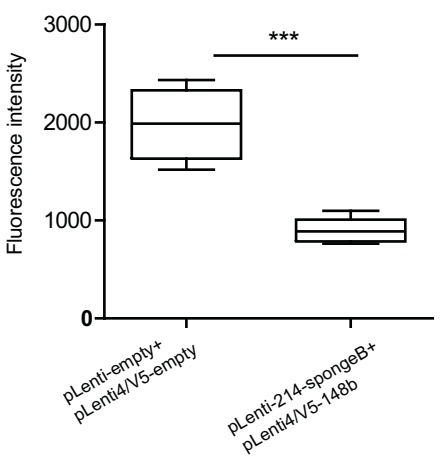
Fluorescence intensity
3000
2000
1000
0
***
pLenti-empty+
pLenti4/V5-empty
pLenti-214-spongeB+
pLenti4/V5-148b

A MA-2

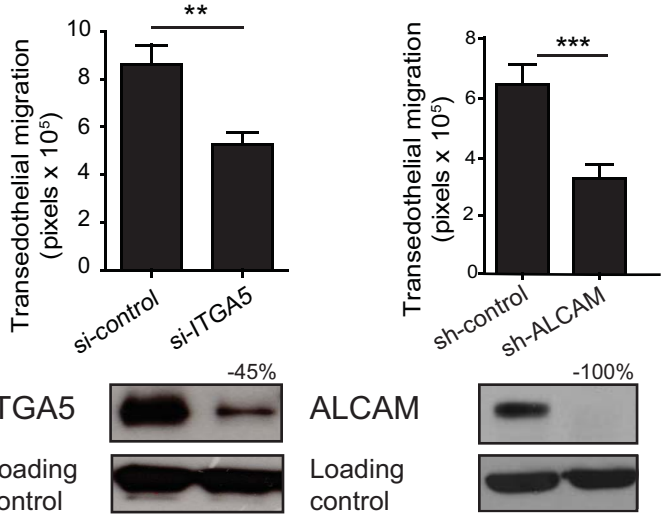

B 4175-TGL

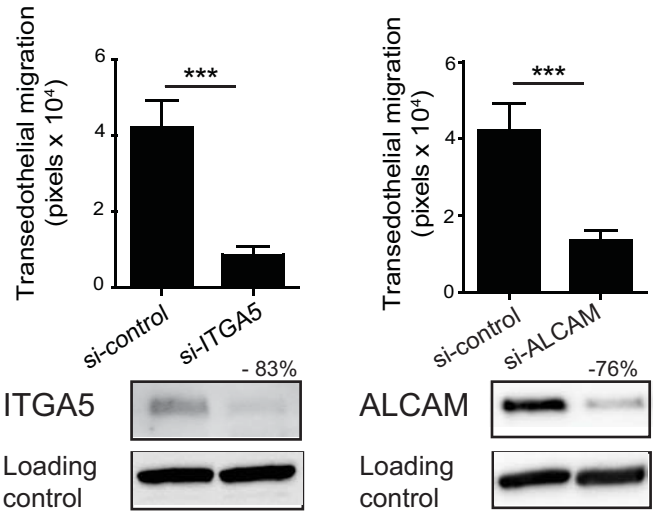

C MA-2

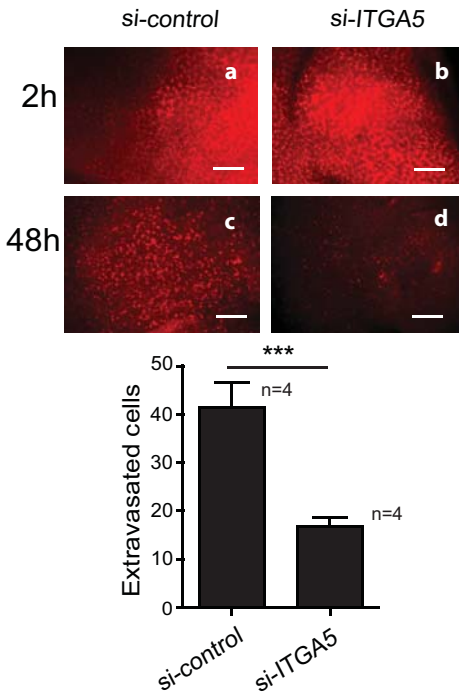

D MA-2

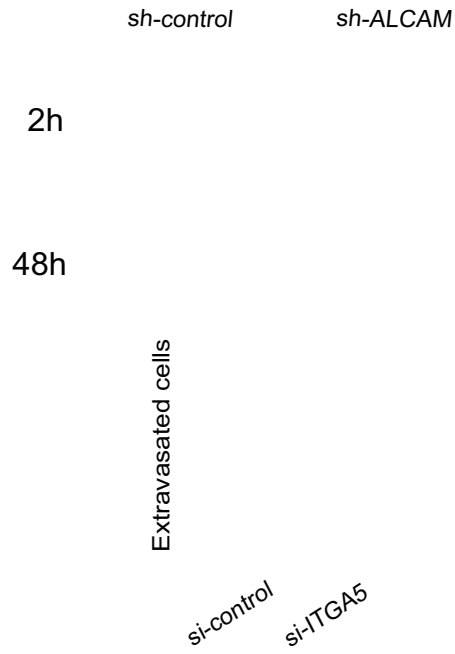

E MA-2

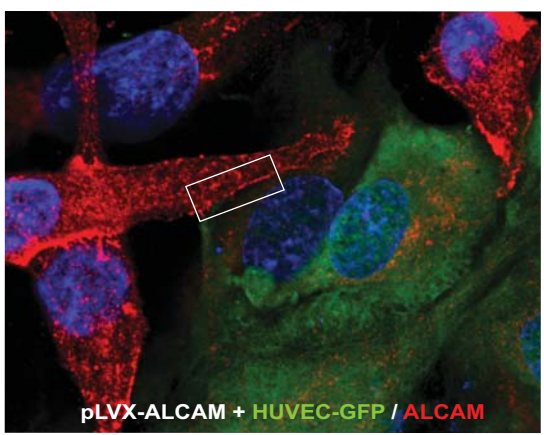

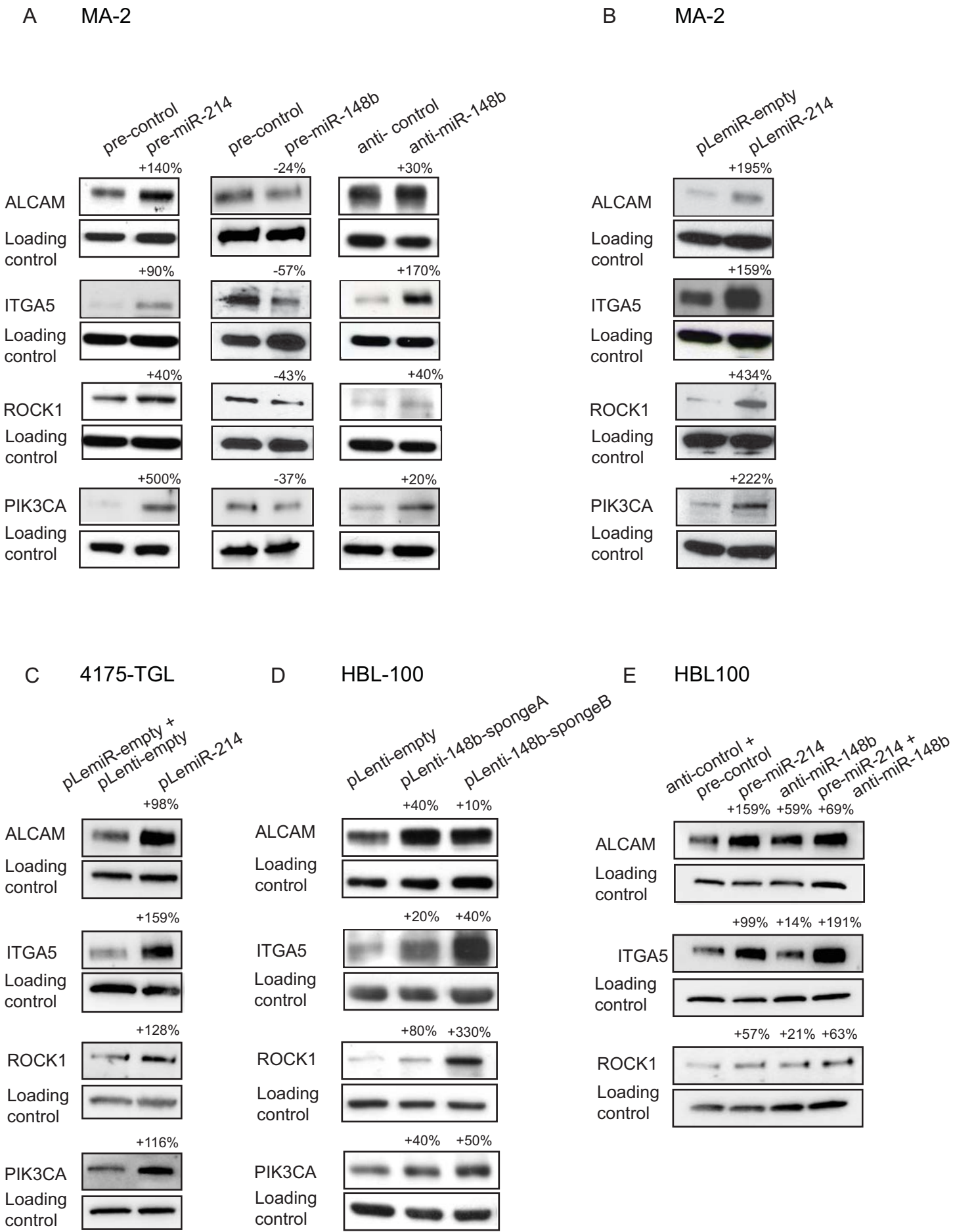
A
MA-2
pre-control
pre-miR-214
pre-control
pre-miR-148b
anti- control
anti-miR-148b
+140%
-24%
+30%
ALCAM
Loading control
+90%
-57%
+170%
ITGA5
Loading control
+40%
-43%
+40%
ROCK1
Loading control
+500%
-37%
+20%
PIK3CA
Loading control
B
MA-2
pLemiR-empty
pLemiR-214
+195%
ALCAM
Loading control
+159%
ITGA5
Loading control
+434%
ROCK1
Loading control
+222%
PIK3CA
Loading control
C
4175-TGL
pLemiR-empty + pLenti-empty
pLemiR-214
+98%
ALCAM
Loading control
+159%
ITGA5
Loading control
+128%
ROCK1
Loading control
+116%
PIK3CA
Loading control
D
HBL-100
pLenti-empty
pLenti-148b-spongeA
pLenti-148b-spongeB
+40%
+10%
ALCAM
Loading control
+20%
+40%
ITGA5
Loading control
+80%
+330%
ROCK1
Loading control
+40%
+50%
PIK3CA
Loading control
E
HBL100
anti-control + pre-control
pre-miR-214
anti-miR-148b
pre-miR-214 + anti-miR-148b
+159%
+59%
+69%
ALCAM
Loading control
+99%
+14%
+191%
ITGA5
Loading control
+57%
+21%
+63%
ROCK1
Loading control